

**Intestinal Immunolocalization and Insight on the Role of Tachykinin-Related
Peptides in the Yellow Fever Mosquito, *Aedes aegypti***

Zeynab Kohandel

A THESIS SUBMITTED
TO THE FACULTY OF GRADUATE STUDIES
IN PARTIAL FULFILLMENT OF THE REQUIREMENTS
FOR THE DEGREE OF MASTER OF SCIENCE

GRADUATE PROGRAM IN BIOLOGY
YORK UNIVERSITY
TORONTO, ONTARIO

December 2023

©Zeynab Kohandel 2023

Abstract

This study investigates a family of neuropeptides known as tachykinin-related peptides (TKRPs) in the mosquito *Ae. aegypti*, which is an insect of medical concern owing to its transmission of several arboviruses. As knowledge on TKRPs is limited in this mosquito, this study aimed to create a *tk* knockout line using CRISPR/Cas9 and characterize the distribution of TKRP immunoreactivity in the midgut over different physiological conditions including starved, sucrose-fed and blood-fed, and across developmental stages. The results demonstrate that TKRP immunoreactivity in the *Ae. aegypti* midgut is greatest in adult stage mosquitoes. Further, starvation significantly reduced TKRP immunoreactivity in the midgut compared to sugar fed adult mosquitoes, but no change was observed in relation to blood-feeding by females. Overall, this study established the intestinal distribution of TKRPs in *Ae. aegypti* and identified functional sgRNAs to disrupt the *tk* gene so that the physiological role of TKRPs can soon be characterized.

Acknowledgement

I would like to express my heartfelt gratitude to the individuals who have supported and guided me throughout my master's thesis journey. Their invaluable assistance and encouragement have been instrumental in the successful completion of this research.

First and foremost, I extend my deepest appreciation to my dedicated supervisor, Dr. Jean Paul Paluzzi. His unwavering guidance, profound knowledge, and continuous support have been the cornerstone of my research. Without his expertise and mentorship, this thesis would not have been possible.

I want to extend a heartfelt thank you to my incredible lab mates and friends: Farwa, Jinghan, Marishia, Salwa, and Britney who have supported me throughout my master's journey. Your patience, willingness to answer all my questions, no matter how "stupid" they may have seemed, and your continuous help with every aspect of my research have been immeasurable.

I would like to acknowledge my advisor, Dr. Raymond Kwong, for his guidance and support throughout this academic journey. His expertise and advice have been invaluable in shaping my research.

I am deeply thankful to Dr. Ben Matthews at UBC and his lab members, Ivan and Cassidy, for their invaluable assistance and guidance in learning embryonic injection techniques. My month-long experience in their lab was a crucial component of my research, and I am truly grateful for their hospitality and expertise.

In addition, I want to express my heartfelt thanks to my parents and my loving sister, who have been my pillars of support from afar. Your unwavering belief in me has been a constant source of strength.

To my wonderful friends and my loving boyfriend here, I cannot thank you enough for your unwavering support and encouragement. Your belief in me and your presence in my life have been a continuous source of motivation and comfort.

To all of you, I extend my deepest gratitude for your indispensable contributions to my academic and personal growth. Your love, encouragement, and belief in me have been the foundation of my success, and I am genuinely thankful for the privilege of having you in my life.

Table of Contents

Abstract.....	II
Acknowledgement	III
Table of Contents.....	IV
List of Tables	VI
List of Figures	VII
1. Introduction.....	1
1.1.The mosquito <i>Aedes aegypti</i> as an important insect to study.....	1
1.2. <i>Aedes aegypti</i> midgut.....	5
1.3.Neuropeptides.....	7
1.4.Tachykinin and Tachykinin related peptides.....	10
1.5.CRISPR/Cas9.....	15
1.5.1. Genome editing techniques.....	15
1.5.2. Cas9: a genome-editing RNA-guided nuclease.....	18
1.5.3. CRISPR/Cas9 in arthropods.....	19
1.6.Research objectives and hypotheses	24
2. Materials & Methods.....	27
2.1.Mosquitoes.....	27
2.2.Immunohistochemistry.....	27
2.3.Starvation assay.....	28
2.4.Blood feeding assay.....	28
2.5.Transforming plasmids into bacteria and protein expression induction.....	29
2.6.Protein purification.....	30
2.7.Coomassie blue staining and immunoblot assay.....	30
2.8.Female injection and dissection.....	31
2.9.sgRNA design, synthesis, and purification.....	32
2.10. Preparing the injection mix	35
2.11. Embryonic microinjection.....	35
2.12. HotSHOT genomic DNA extraction and screening by genotyping, heteroduplex mobility and mixed heteroduplex mobility assay.....	38
2.13. Colony PCR of pGEM-T Easy vector.....	40
2.14. Statistical analysis.....	40
3. RESULTS.....	41
3.1.Optimization of injection conditions (ReMOT).....	41
3.2.Determining the best sgRNA candidate and embryonic microinjection.....	50

3.3.Immunolocalization of TKRPs in the midgut of the mosquito <i>Ae. aegypti</i> over different developmental stages and under various physiological conditions including blood fed, sucrose fed and starvation.....	52
4. Discussion.....	59
4.1. <i>tk</i> knockout <i>Ae. aegypti</i> line generation using CRISPR/Cas9.....	59
4.1.1. ReMOT Control.....	61
4.1.2. Embryonic microinjection.....	63
4.2.Midgut as one of the major sources of TKRP production in <i>Ae. aegypti</i> through development.....	64
4.3.Immunoreactivity distribution of TKRP in different physiological conditions including blood feeding, developmental stage, and starvation.....	65
4.4.Concluding remarks and future directions.....	67
References.....	68

List of Tables

Table 2.1 sgRNA oligos and genome screening primers.....	33
Table 3.1 Testing out sgRNAs to find the best sgRNA candidate.....	55

List of Figures

Figure 1.1 Developmental stages of <i>Ae. aegypti</i> depicted schematically. There is an aquatic phase (larvae, pupae) and a terrestrial phase (eggs, adults).....	4
Figure 1.2 An illustration of the alimentary canal of an adult mosquito.....	6
Figure 1.3 CRISPR/Cas9 gene editing technique and delivery strategy utilising embryonic microinjection.....	22
Figure 1.4 CRISPR/Cas9 gene editing technique and delivery strategy utilising ReMOT control.....	23
Figure 2.1 Six different sgRNAs and two primer sets.....	34
Figure 2.2 Embryonic microinjection.....	37
Figure 2.3 Heteroduplex mobility and mixed heteroduplex mobility assay.....	39
Figure 3.1 Immunohistochemistry on the anterior midgut of homozygous mutants (left side) and wildtype (right side) adult 1 day old mosquitoes.....	43
Figure 3.2 Localization of TKRP in the midgut of adult mosquito <i>Ae. aegypti</i>	44
Figure 3.3 Schematic diagram of the midgut of 4 th instar larval stage (a) and 1 day old adult (b) <i>Ae. aegypti</i> mosquito TKRP immunoreactivity.....	45
Figure 3.4 Immunohistochemistry on 4 th larval stage of the mosquito <i>Ae. aegypti</i>	46
Figure 3.5 Immunohistochemistry on different aged adult mosquitoes.....	47
Figure 3.6 Immunohistochemistry on blood fed and non-blood fed adult mosquitoes.....	48
Figure 3.7 Immunohistochemistry on starved (left side) and sugar fed (right side) mosquitoes..	49
Figure 3.8 Cell counting of the immunohistochemistry anterior midgut images of adult female mosquitoes and 4 th instar larvae.....	51
Figure 3.9 P2C-EGFP-Cas9 recombinant protein uptake into ovaries following injection.....	54
Figure 3.10 Finding the best sgRNA candidate screening.....	56
Figure 3.11 G1 sequencing.....	57
Figure 3.12 Homozygous mutant screening.....	58

1. Introduction

1.1. The mosquito *Aedes aegypti* as an important insect to study

The vector mosquito *Ae. aegypti* (Diptera: Culicidae) has significant medical importance as they transmit several pathogenic agents to humans (Raminani and Cupp 1975; Watts et al. 1987). This species is widespread in most tropical and subtropical parts of the planet, with a cosmopolitan distribution between 20° S and 30° N latitudes (Powell and Tabachnick, 2013) that demonstrates a liking for human environments with standing water in these areas. Adult *Ae. aegypti* mosquitoes are medium-sized insects that measure 4–7 mm in length and resemble the Asian tiger mosquito, *Ae. albopictus*. Adults have a dark brown to black abdomen that may contain white scales and a dorsal side of their thorax that is covered in white scales. The tarsal segments of the hind legs feature white basal bands that resemble stripes (Powell and Tabachnick, 2013).

Both males and females consume plant nectar, but for successful oviposition, females have piercing and sucking mouthparts designed for acquiring meals of vertebrate blood. Females typically blood-feed on human hosts around dusk and dawn. Adult females may lay 100–200 eggs per batch and can generate up to five batches of eggs throughout their lives. Eggs may withstand desiccation for several months even though they are normally placed on moist surfaces (Clemons et al., 2010). In temperate areas, mosquitoes of the tribe *Aedine* often overwinter in the diapause egg stage, which is resistant to freezing and lasts until spring when they emerge as larvae (Clemons et al., 2010).

The *Ae. aegypti* mosquito undergoes complete metamorphosis during its life cycle with four unique life stages: egg, larva, pupa, and adult (Figure 1.1). The presence of water and the

surrounding temperature have a direct impact on their growth cycle. A little over a week is needed for the development of eggs into adults on warm days with temperatures about 25°C. Development may take many months to complete in the event of chilly days (Lopes et al., 2014). The pupal stage and all four larval stages are aquatic (Figure 1.1). Although larvae swim below the surface when they feed on organic particulate matter such as algae and other tiny creatures in their aquatic environments, the majority of the larval stages, which span at least four days, are spent above the water surface due to the need to breathe. Following the fourth instar, *Ae. aegypti* go into a non-feeding, two-day-long pupal stage that is mobile (Figure 1.1). Depending on the surrounding environment, this insect has an adult life span that can range from two weeks to a month or more (Christophers, 1960; Clements and Clements, 1992).

Due to its role in the spread of pathogens leading to illnesses, *Ae. aegypti* is commonly known as the yellow fever or dengue fever mosquito. Resultantly, it is of significant medical concern as a vector of dengue virus, yellow fever virus, chikungunya virus, and Zika virus (Kauffman and Kramer, 2017). *Ae. aegypti* has also been proposed as a possible vector for the Venezuelan Equine Encephalitis virus and research on its vector competency demonstrated its capacity to spread West Nile virus (Christophers, 1960). While *Ae. aegypti* had evaded designation as a global species until 1900, several collections of this species from various tropical locales were documented after the discovery that this and other mosquitoes transmit human illness (Christophers, 1960). *Ae. aegypti* is the chief carrier of yellow fever virus, infecting 200,000 people annually and killing 30,000 per year. Tropical areas of Africa and parts of South America are where yellow fever is most common. From a self-limited febrile sickness to acute hepatitis with hemorrhagic fever, this condition can be severe (Kauffman and Kramer, 2017). Additionally, *Ae. aegypti* is the main mosquito vector responsible for the spread of dengue virus infections, which

can cause dengue fever, a nonspecific febrile illness that is the most prevalent and serious arboviral disease in the world (Clemons et al., 2010). To spread disease, a female mosquito must bite an infected individual and, following a time of viral incubation within the insect, then bite and infect another human. Female mosquitoes employ signals such as odour, carbon dioxide, and temperature to identify a host and obtain a blood meal, which is necessary to generate a clutch of roughly 100-200 eggs (McMeniman et al., 2014). Once mature eggs have been developed, a mosquito utilises volatile and touch signals to identify and assess a body of water in which to lay her eggs (Kistler et al., 2015).

Ae. aegypti has undergone a wide range of laboratory investigations due to the relative ease with which it can be raised in culture, including analysis of its morphology, physiology, genetics, vector competence, and molecular evolution (Clements and Clements, 1992). In particular, *Ae. aegypti* analysis has shed light on the study of mosquito/pathogen interactions in great detail. After consuming blood from an infected host, the pathogen must endure internal defence processes designed to identify and eliminate alien organisms (Clemons et al., 2010). It is crucial to examine vector competence in mosquito species with well-characterized genetic profiles, such as *Ae. aegypti*, because genetic variations are responsible for variation in vector competence (Chen et al., 2008; Clemons et al., 2010). Utilising *Ae. aegypti* allowed for the genetic investigation of the dengue vector competence base as well as serving as a model for the genetic underpinnings of vector competence for malaria parasites, even though it is not a vector for human malarial parasites (Clemons et al., 2010; Soghigian et al., 2020). Instead, it is a vector for the avian malarial parasite, *Plasmodium gallinaceum*. The Liverpool strain of *Ae. aegypti* is also susceptible to the human-infecting filarial nematode strains *Brugia malayi* and *Wucheria bancrofti*, despite the fact that *Ae. aegypti* is not a natural vector for lymphatic filariasis (Severson et al., 2004). As a result, *Ae. aegypti*

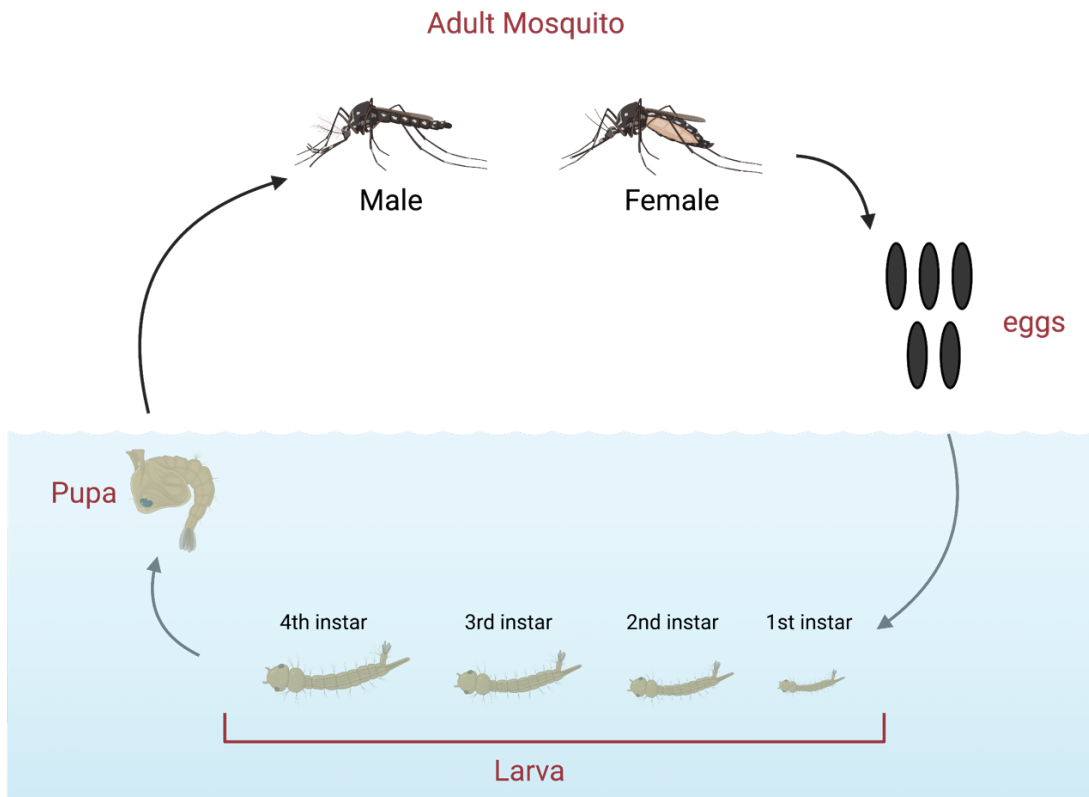


Figure 1.1: Developmental stages of *Ae. aegypti* depicted schematically. There is an aquatic phase (larvae, pupae) and a terrestrial phase (eggs, adults). The insect undergoes complete metamorphosis, going through the stages of egg, larva, pupa, and adult. The lifespan of an adult might vary based on the surroundings from two weeks to a month. The *Aedes aegypti* life cycle can last between one and a half to three weeks. Figure was created using BioRender.com.

can also serve as a model for the genetics of filarial worm vector competence (Clemons et al., 2010).

1.2. *Aedes aegypti* midgut

The midgut is where the blood meal of haematophagous insects is digested, and this organ also starts blood-feeding-related processes including vitellogenesis, oogenesis, and pathogen transmission (Billingsley and Lehane, 1996). Midgut cells actively form the microbiome, establish innate immune defences against harmful microbes, and create signaling molecules to control their own physiology as well as the physiology of other mosquito organs (Caccia et al., 2019). The first organ to contract an arbovirus is the midgut of the female mosquito. Two significant hurdles to systemic arbovirus infection that affect the ability of a mosquito to transmit a virus are midgut infection and escape barriers (Cui and Franz, 2020). Anatomically, the anterior and posterior midgut regions are the two primary areas of the mosquito midgut, which is an elongated tube-like organ (Billingsley and Lehane, 1996) (Figure 1.2). Notably, there is partitioning of ingested food stuffs and its digestion within the alimentary canal of *Ae. aegypti*. For example, meals containing sugar that are initially stored in the crop are predominantly digested by the anterior midgut whereas digestion of the blood meal is a speciality of the posterior midgut. The single-layered epithelium of the midgut organ is bordered by muscle cells, tracheoles, and fibroblasts, which are all encased in an extracellular matrix made of banded collagen fibrils (Cui and Franz, 2020).

Due to the digestion of blood meals and associated hormone signaling, the mosquito midgut is crucial for nutrition processing and absorption as well as female fertility (Sanders et al., 2003). The mosquito midgut is also a crucial organ in defining the vector competence for arboviruses in

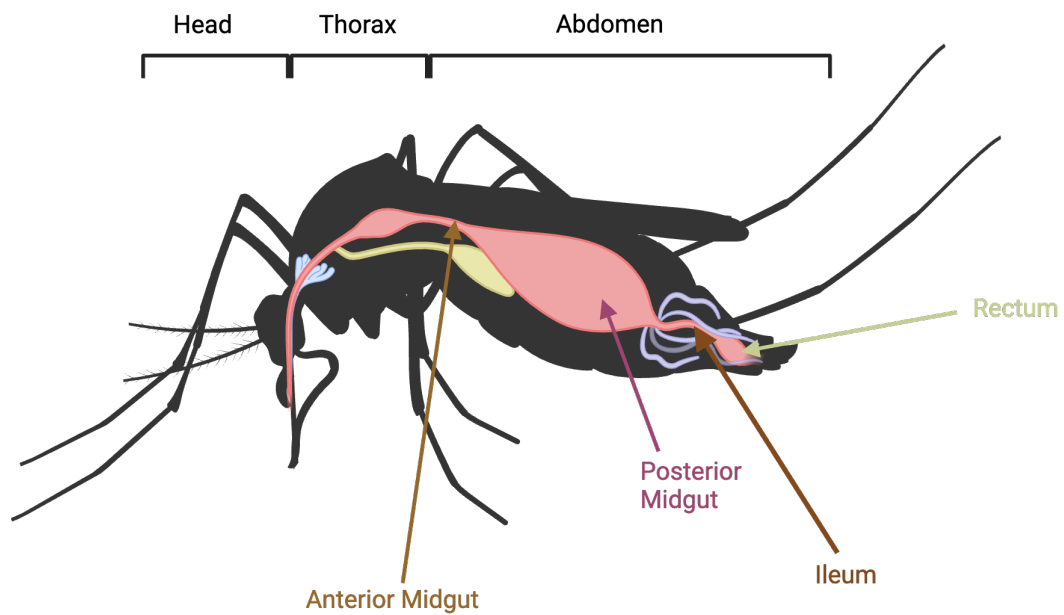


Figure 1.2: An illustration of the alimentary canal of an adult mosquito. The head, thorax, and abdomen are the three main body segments. The midgut is the elongated tube-like organ which is divide into two region: anterior midgut and posterior midgut. These two organs are different in shape and function, but both have roles in digestion. The hindgut and Malpighian tubules are the primary excretory organs of adult mosquitoes. Figure was created using BioRender.com.

culicine mosquitoes like *Ae. aegypti*. Over the past few decades, a plethora of knowledge has been produced on the physiology, biochemistry, and molecular biology of the whole mosquito midgut. For instance, it has been demonstrated that ingesting a blood meal produces significant structural changes in the midgut epithelium of the female mosquito (Cui and Franz, 2020). Additionally, ingesting blood meals has a significant impact on the transcriptome and proteome of the mosquito midgut (Cui and Franz, 2020)

1.3. Neuropeptides

The nervous system of most, if not all, animal phyla has a wide and varied collection of intercellular signaling molecules called neuropeptides (Hökfelt et al., 2018; Larhammar, 2009), which are short chains of amino acids that neurons or endocrine cells produce and release as chemical messengers. Most often, neuropeptides target G protein-coupled receptors (GPCRs) to influence the function of the nervous system as well as other tissues like the heart, muscles, and gut (Caers et al., 2012). In humans, over 100 neuropeptides have been identified, making them the largest and most diverse class of signaling molecules in the nervous system (Mains and Eipper, 1999). Large precursor proteins are post-translationally processed before being bundled into dense core vesicles to become biologically active neuropeptides. In a single neuron, neuropeptides are frequently co-released with other neuropeptides and neurotransmitters, producing a variety of effects. Neuropeptides can diffuse broadly after release and have an impact on a variety of target tissues often at a distance from their site of origin (Bhat et al., 2021; Elphick et al., 2018).

Neuropeptides are synthesised in the cell soma, then sequestered inside the lumen of the secretory channel and transported down the axon while undergoing cleavages and other post-translational processing activities, after which the peptide-containing, large dense core vesicle

(LDCV) is utilised once (Altstein and Nässel, 2010; Elphick et al., 2018). The membrane components of the LDCV must be reinternalized after exocytosis and then transported to the cell body, where they can either be destroyed or used again (Altstein and Nässel, 2010). Prepropeptides, are the precursor proteins from which neuropeptides are derived (Hansen et al., 2010; Nässel, 1999; Pauls et al., 2014). The components of prepropeptides are a signal peptide, which directs the protein to the secretory pathway, progenitors of mature peptides, or the biologically active peptides, spacer peptides, which are non-conserved peptide fragments that often have unknown biological functions, and monobasic and dibasic cleavage sites (Altstein and Nässel, 2010; Nässel et al., 2019; Purves et al., 2001). One or more mature neuropeptides or peptide hormones can be produced from each precursor. Different insect species create different numbers of mature peptides from one or multiple precursors, or can create different peptides from one precursor (Caers et al., 2012; Larhammar, 2009). These can be either a group of extremely similar peptides with mostly conserved sequences and hence comparable receptor activation capabilities such as tachykinin-related peptides (TKRP) and FMRFamides (Nachman et al., 1999; Nässel et al., 2019). Alternatively, peptides with different sequences and activities, such as those derived from the *capability* gene (CAPA) and *vasopressin* gene, which are examples of precursors with diverse peptide sequences and functions, as they bind separate receptors (Bhat et al., 2021; Kahsai et al., 2010). Additionally, gene paralogs and splice variants of a single gene have been shown to create peptides with comparable sequences. For example, up to 38 paralogous genes in the silk moth *Bombyx mori* and 8 genes in *D. melanogaster* encode insulin-like peptides (Mizoguchi and Okamoto, 2013). Comparatively, by alternative splicing, the orcokinin gene in insects creates two distinct neuropeptide precursors: orcokinin A and orcokinin B (Wulff et al., 2018).

The molecular identification of neuropeptides in invertebrates, such as adipokinetic hormone (AKH) and proctolin in insects (Sehadova et al., 2020), and the molluscan cardioexcitatory neuropeptide FMRFamide (Cottrell et al., 1984), revealed evidence of the evolutionary antiquity of neuropeptide signaling. In addition, research using various antibodies against vertebrate neuropeptides demonstrated immunoreactivity in invertebrates (Curry et al., 1989; Veenstra, 1988). The sequencing of neuropeptides isolated from invertebrates with similarities to those described in vertebrate species provided solid confirmation of the vast phylogenetic distribution and ancient evolutionary origin of several neuropeptide families by the late 1980s (Fónagy et al., 1992). A cholecystinin-type neuropeptide (Nachman et al., 1986) and vasopressin/oxytocin (VP/OT)-type neuropeptide (Satake et al., 1999) were discovered in insects. However, it wasn't until the turn of the century that it was possible to thoroughly investigate the relationships between neuropeptide systems in vertebrates and invertebrates thanks to the sequencing of the genomes of the nematode, *Caenorhabditis elegans*, the insect *D. melanogaster*, and *Homo sapiens* (Adams et al., 2000; Noonan et al., 2006; Whitton et al., 2004).

In many animals, including mosquitoes, neuropeptides undergo a remarkable transformation—they are converted, stored, and released as neurotransmitters or neuromodulators within the nervous system. Additionally, they function as circulating hormones when released from the peripheral nervous system, central nervous system (CNS), or midgut and other endocrine organs. To connect with their intended targets and carry out their functions, these peptide messengers primarily interact with membrane receptors, to a lesser extent, receptor tyrosine kinases (Predel et al., 2010). For *Ae. aegypti*, which is regarded as the most tractable mosquito species for physiological and endocrine investigations, the transcript, processed peptide, and functional role of numerous neuropeptides and protein hormones have been characterised,

including head peptides (Matsumoto et al., 1989), insect kinins (Veenstra, 1994), allatostatins (AST-A) (Veenstra et al., 1997), ovarian ecdysteroidogenic hormone (OEH) (Brown et al., 1998), allatotropin (AT) (Veenstra and Costes, 1999), ecdysis triggering hormone (ETH) (Dai and Adams, 2009), and adipokinetic hormone (AKHs) (Kaufmann and Brown, 2006). Relatedly, the neuropeptides corazonin (CRZ), AKH/CRZ-related peptide (ACP), and AKH are thought to be similar to the vertebrate gonadotropin-releasing hormone (GnRH). Wahedi et al. 2019 showed how, despite having a very high degree of ligand and receptor homology, two GnRH-related systems in *Ae. aegypti* sharing the most recent evolutionary origin, function independently with no receptor cross activation by members of the related peptide family (Wahedi et al., 2019).

1.4. Tachykinin and Tachykinin related peptides

According to several studies, neuropeptides frequently function at synaptic locations as co-transmitters with tiny molecules that are rapid transmitters (Hökfelt et al., 2018; Nässel et al., 2019). Only a few studies have really shown co-transmitter activities in invertebrates because neuropeptides are typically thought of as neuromodulators in these organisms (Altstein and Nässel, 2010; Nässel et al., 2019). Notably, a single neuropeptide can function as a co-transmitter, neuromodulator, and neurohormone. Tachykinin-type peptides (TKs), which are produced by interneurons, neuroendocrine cells of the central nervous system (CNS), and intestinal endocrine cells, provide an illustration of this in *D. melanogaster* (Ignell et al., 2009; Nässel, 1999). Thus, TKs are involved in a variety of neuronal circuits and are occasionally co-expressed with other neuropeptides or the rapid neurotransmitter molecule γ -aminobutyric acid (GABA) (Glantz et al., 2000). TKs also appear to act through both endocrine and paracrine signaling, meaning they act at a distance and on adjacent or nearby cells, respectively, following release (Song et al., 2014).

In mammals, one of the most well investigated neuropeptide families are the TKs, which include substance P that was the first member of this family to be identified nearly a century ago (Champagne and Ribeiro, 1994; Nässel et al., 2019; v. Euler and Gaddum, 1931). They are made up of a group of peptides with similar primary structures that result from the alternative processing of three *Tac* genes and are produced throughout the immune and nervous systems. Three G protein-coupled receptors for neurokinins are activated by tachykinins (Nässel et al., 2019). Extensive research has also been done on the signaling, trafficking, and regulation of neurokinin receptors (Mishra and Lal, 2021; Steinhoff et al., 2014). TKs have a crucial role in several physiological processes, such as inflammation, nociception, smooth muscle contraction, epithelial secretion, and proliferation, in the neurological, immunological, gastrointestinal, respiratory, urogenital, and cutaneous systems (Nässel, 1999; Steinhoff et al., 2014; Urbański et al., 2022). TKs contribute to multiple disease-related processes including acute and chronic inflammation and pain, fibrosis, emotional and addiction disorders, functional problems of the gut and urinary bladder, infection, and cancer (Nässel et al., 2019; Severini et al., 2002).

From Cnidaria to vertebrates, TKs are one of the most conserved neuropeptide families. Tachykinin-related peptides (TKRPs) are a family of neuropeptides that are found in insects that have structural similarities to TKs and play roles in the control of several processes (Nässel et al., 2019). Recent findings also suggest that TKRPs play a significant role in hormonal axes, which are essential for insects to respond to stressful situations (Caers et al., 2012; Kahsai et al., 2010). The regulatory function of these hormones is primarily dependent on the status and activity of the insect immune system as well as the adaptation of insect metabolism to the present physiological condition (Caers et al., 2012; Kahsai et al., 2010). Despite the well-known immunotropic abilities

of AKHs and ILPs (Dolezal et al., 2019; Zhang et al., 2018), we know relatively little about the function of TKRPs in this regard.

The insect TKRPs are found in various species in a number of closely similar forms, much like in mammals (Helke et al., 1990). The locust, *Locusta migratoria*, has five TKRPs (named locustatachykinins I–V; LomTK-I–V) (Schoofs et al., 1990a; Schoofs et al., 1990b). In the brain and midgut of the cockroach *Leucophaea maderae*, nine TKRP isoforms were discovered (Muren and Nässel, 1996). Similar to the LomTKs, these peptides, referred to as LemTRP-1-9, are distinguished by a conserved carboxy terminal hexapeptide composed of -GFX₁GX₂Ramide (where X₁ is F, H, L, M, Q or Y and X₂ is M, T or V). The LemTRPs have variable amino termini, and the isoform lengths range from 9 to 19 amino acid residues. Three LemTRPs were discovered in both the brain and midgut, whereas four LemTRPs appeared to be exclusive to the brain, while two LemTRPs were only found in the midgut (Muren and Nässel, 1996). Thus, it appears that the cockroach expresses at least a subset of TKRPs in a tissue-specific manner similar to mammals (Helke et al., 1990).

The sequences of TKRPs from the more distantly related mollusc and worm species differ substantially from TKRPs isolated from the crab *Cancer borealis* (CabTRP-Ia and Ib), which are relatively similar to the cockroach peptides (Christie et al., 1997). Despite sequence variations, every invertebrate TKRP discovered so far acts as a stimulant of spontaneous contractions on the hindgut of cockroach (Christie et al., 1997). An antiserum produced to the locust peptide LomTK-I can be used to demonstrate the presence and distribution of TKRP immunoreactivity (Christie et al., 1997). As a result, the distribution of TKRPs in various invertebrates have been mapped using immunohistochemistry. In the brains of insects and crustaceans, the patterns of neuronal dispersion of TKRPs have been rather well conserved (Nässel et al., 2019).

Several invertebrates have had their TKRPs isolated. Both invertebrate TKRPs (FX₁GX₂Ramide) and peptides that are obviously linked to vertebrate tachykinins (FXGLMamide) such as sialokinins I and II from mosquitoes (Champagne and Ribeiro, 1994) and eledoisin (Severini et al., 2002) from cephalopods, are two of the primary categories. Sialokinins are tachykinins of the vertebrate type that were isolated from salivary glands of mosquitoes (Champagne and Ribeiro, 1994). On the other hand, the salivary glands do not have the invertebrate variety of TKRPs. The nervous system and gut both express TKRPs (Holzer and Holzer-Petsche, 1997; Muren and Nässel, 1996). The cockroach *L. maderae* has the most similar variants that have been found (Muren and Nässel, 1996; Muren and Nässel, 1997). Nine or ten distinct TKRPs, known as LemTRPs as discussed earlier, were so far isolated from this insect species. The sequence of the tenth version of LemTRP-10 differs somewhat from that of the other LemTRPs, and it is not C-terminally amidated. Several cockroach isoforms were extracted in amounts ranging from 140 to 780 fmol per brain (Muren and Nässel, 1996). It was believed that other cockroach isoforms would be identified through molecular cloning along with more isoforms in the mosquito, blowfly, and locust (Schoofs et al., 1990b).

More than 160 TKRP-expressing neurons may be classified into 11 bilateral groups and one unique pair in the adult *D. melanogaster* brain, according to *in situ* hybridization and immunolabeling results (Winther et al., 2006). Ion transport peptide (ITP), short neuropeptide F (sNPF), and TKRP are co-expressed by ten large lateral neurosecretory cells (ITPn) (Kahsai et al., 2010). The remaining TKRP neurons are interneurons of various types that innervate the subesophageal zone, pars intercerebrum, antennal lobes, optic lobes, and the fan-shaped body of the central complex (Winther et al., 2006).

Although there are far more TKRP neurons in the brains of the cockroach *L. maderae* and the locust *L. migratoria*, the innervation pattern of the various brain areas is comparable to that of *D. melanogaster* and the moth, *Spodoptera litura* (Nässel et al., 2019). Roughly 360 TKRP-positive neurons were discovered in the *L. maderae* brain (without optic lobes) (Muren and Nässel, 1997), and roughly 800 were discovered in the complete *Locusta migratoria* brain (Nässel, 1999). In contrast to *D. melanogaster*, cockroaches have widespread axon terminations over the foregut and midgut as well as motor neurons in the stomatogastric ganglia, also known as efferent TKRP neurons, that innervate the hindgut and regulate motility of the foregut and gut. They also transmit signals from the brain to the peripheral nervous system, triggering an action (Muren and Nässel, 1996; Muren and Nässel, 1997).

TKRPs in the hemipteran blood-sucking bug, *Rhodnius prolixus*, has also been extensively studied. In the brain of *R. prolixus*, over 250 TKRP immunoreactive neurons were discovered (Kwok et al., 2005). These are dispersed in the optic lobes and many other clusters. Contrary to many other researched insects, this species has no enteroendocrine cells that contain TKRP, although TKRP immunoreactive axons from the abdominal ganglia innervate the hindgut (Kwok et al., 2005). Another myostimulatory peptide, leucokinin, is expressed in these TKRP immunoreactive axons. The salivary gland in *R. prolixus* is a tissue that exhibits high levels of TKRP mRNA but with no TKRP immunoreactivity. Interestingly, *R. prolixus* TKRPs were demonstrated to enhance the basal tonus of the hindgut as well as the frequency and amplitude of peristaltic contractions of the salivary gland (Kwok et al., 2005).

In the mosquito *Ae. aegypti*, four different transcript variants produce TKRPs (Nene et al., 2007; Predel et al., 2010), which for the most part, yield the same peptides; however, two out of the four transcript variants, do not produce the fifth TKRP peptide. The *Drosophila* tachykinin-

related peptides (DTKs-1 through 6) are all produced by the same precursor encoded by the *Tk* gene (CG14734). DTKs are abundantly dispersed in the midgut endocrine cells and CNS interneurons (Poels et al., 2009). Earlier studies have provided some insight into the distribution of TKRPs in the *Ae. aegypti* mosquito investigating their immunolocalization and peptide mapping. Antiserum to locustatachykinin 2 labelled endocrine cells in the anterior midgut, as well as in the most frontal and caudal regions of the posterior midgut (Veenstra et al., 1995). Moreover, neuropeptidomic studies of the mosquito *Ae. aegypti* have shown the presence of TKRPs in the dorso-caudal neuropil (DCN) of the terminal ganglion as well as anterior and posterior parts of the midgut (Predel et al., 2010).

1.5.CRISPR/Cas9

The ability to create customized biological systems and creatures holds enormous potential in biotechnology, medicine, and fundamental science. Programmable sequence specific endonucleases have made it possible to carry out precise edits on endogenous genomic loci systematically across a wide range of species, even those that were genetically untraceable before (Ran et al., 2013).

1.5.1. Genome editing techniques

Genome editing technologies like Zinc finger nucleases (ZFNs), transcription activator like effector nucleases (TALENs), and RNA-guided CRISPR/Cas nuclease system are currently being used widely in different research fields. The first two techniques involve an attaching process where targeted DNA double stranded breaks (DSBs) are caused at specific genomic loci by

catalytic domains attached to modular DNA binding proteins. On the other hand, Cas9 nuclease is guided into place through small RNAs base pairing with target DNA using Watson Crick connectivity (Hsu et al., 2014; Ran et al., 2013).

The CRISPR/Cas9 system, which is significantly more practical and efficient than ZFNs and TALENs, has lately supplanted these two genome-editing techniques (Lander, 2016; Wang et al., 2016). On the other hand, when compared to RNA interference (RNAi) technology, CRISPR/Cas9 causes stable and heritable changes at the genomic level, and the mutant gene can be passed down to future generations, whereas gene silencing by RNA interference typically occurs temporarily, unless the dsRNA is continuously supplied (Adli, 2018). CRISPR/Cas9 system is significantly simpler to design, highly specific, effective, and well-suited for high-throughput and multiplexed gene editing for a variety of cell types and organisms.

In facilitating efficient genome editing processes, Cas9 creates an essential double-stranded break within specified genomic domains similar to the modes of action of ZFNs and TALENs (Uddin et al., 2020). After initiating such alterations at target loci using Cas9 cleavage technology, there are commonly two primary means through which DNA undergoes damage response mechanisms: high fidelity Homology Directed Repair (HDR) or error prone Non-Homologous End Joining (NHEJ). In instances where a repair template is not accessible, the NHEJ resolution loop often results in insertions or deletions (indels) mutations that usually lead to scars (Wang et al., 2016). Due to frameshift mutations and premature stop codons, indels occurring within coding exons can generate knockouts using NHEJ. Moreover, several DSBs can mediate more extensive deletions throughout genomes (Ran et al., 2013).

HDR offers an alternative yet equally important route for facilitating DNA repair processes. Despite exhibiting lower frequencies than conventional NHEJ, HDR allows targeted sequencing

variations that are both accurate and specific – the caveat being that these alterations are typically accompanied by an externally supplied repair template. This external apparatus can take the form of single strand DNA or double stranded templates containing homologous flanking regions around insertion segments. Using this approach yields significant efficiency gains when dealing with minor genome manipulations such as single nucleotide point-mutations for deducing causative genetic traits leading to unique phenotypic attributes. In contrast to NHEJ, HDR is typically only active in dividing cells, and the genomic locus and repair template, together with the cell type and state, all have a significant impact on the effectiveness of HDR (Hsu et al., 2014; Kistler et al., 2015; Ran et al., 2013).

1.5.2. Cas9: a genome-editing RNA-guided nuclease

Microbes possess remarkable adaptive immune mechanisms called CRISPR-Cas systems that use RNA-guided nucleases to cleave foreign genomic material. Many bacterial and archaeal hosts harbor three types (I-III) of these systems, which comprise CRISPR associated (Cas) genes, noncoding RNAs, and a specific collection of repeated elements called direct repeats (Zhang et al., 2020). The CRISPR RNA (crRNA) array includes repetitions separated with short variable sequences generated from foreign DNA targets known as protospacers. Each protospacer features a protospacer adjacent motif (PAM) inside the DNA target site that may differ depending on the specific CRISPR system (Adli, 2018; Barrangou and Marraffini, 2014; Zhang et al., 2020). One well studied system is Type II that contains Cas9 enzyme, crRNA array encoding guide RNAs, and an auxiliary trans-activating crRNA (tracrRNA). This secondary RNA helps to process the crRNA array into discrete units for efficient targeting (Hammond et al., 2016). The *Streptococcus*

pyogenes derived CRISPR-Cas systems require DNAs with an immediate precedent 5'-NGG PAM motif as their target.

In less than a decade, CRISPR/Cas9 technology has been extensively employed to alter the genome sequences of several species, including animals, plants, and bacteria (Basu et al., 2015; Ran et al., 2013; Zhang et al., 2020). A large portion of these investigations used model organisms, which are non-human species that has undergone considerable research to comprehend specific biological phenomena, with the hope that what is learned about the model organism may help us understand how other organisms function (Baldrige et al., 2021). In recent years, researchers have exploited the CRISPR/Cas9 system by injecting sgRNA and Cas9 into zygotes to modify the genomes of many other organisms, such as cattle (Heo et al., 2015), goats (Ni et al., 2014), pigs (Hai et al., 2014), rabbits (Honda et al., 2015), and malaria parasites (Singer and Frischknecht, 2017). Several studies have summarised the effective use of various genome editing technologies, including the CRISPR/Cas9 system, in arthropods, particularly in insects (Chaverra-Rodriguez et al., 2018; Hammond et al., 2016; Kistler et al., 2015; Macias et al., 2020; Martin-Martin et al., 2018).

1.5.3. CRISPR/Cas9 in arthropods

The CRISPR/Cas9 system, a revolutionary genome editing tool, was first utilized in arthropods using the insect, *D. melanogaster*. In 2013, Gratz et al. used CRISPR/Cas9 to successfully modify the *D. melanogaster* genome, generating knockout and knock-in lines for the *yellow, rosy* gene (Gratz et al., 2013). This scientific achievement established that CRISPR/Cas9 can successfully modify the *D. melanogaster* genome.

Researchers expanded the application of CRISPR/Cas9 to more arthropod species in light of the success obtained in the fruit fly. The silkworm, *Bombyx mori*, was the next arthropod to have access to CRISPR/Cas9 technology. This technique was used to demonstrate the viability of CRISPR/Cas9 for genome editing by exploiting the phenotypic effects of gene mutations in silkworms (Wang et al., 2013). The CRISPR/Cas9 method was then used on a variety of non-traditional model insects, such as mosquitoes (Dong et al., 2015; Kistler et al., 2015), moths (Wang et al., 2013), butterflies, and other arthropods that are not flies . Due to the growing use of CRISPR/Cas9 and the accessibility of organised genomic resources, comparative research between various species has been made easier.

In the mosquito *Ae. aegypti*, two of the successful methods for employing CRISPR/Cas9 include embryonic microinjection (Kistler et al., 2015) and Receptor-Mediated Ovary Transduction of Cargo (ReMOT Control) (Chaverra-Rodriguez et al., 2018). Any CRISPR gene editing application must successfully deliver Cas9 endonuclease and sgRNAs to the appropriate tissue at the right time. To achieve this, a variety of approaches have been tested for delivering the Cas9 endonuclease and sgRNA to mosquitoes, including direct injection of the sgRNA and Cas9 (as either mRNA or protein) or crossing genetically encoded sgRNA-expressing mosquitoes with Cas9-expressing mates to produce offspring endowed with the ability to self-edit (Kistler et al., 2015; Martin-Martin et al., 2018).

In the direct delivery method, Cas9/sgRNA components are injected into early mosquito embryos, known as the pre-syncytial blastoderm stage, when the embryo is one giant multinucleated cell (Sun et al., 2022) (Figure 1.3). For this approach, either pure Cas9 mRNA or recombinant Cas9 protein can be utilised. Insertion of the donor DNA into the cut site by HDR is also possible if donor DNA (such as short single-stranded DNA oligonucleotides [ssODN] or

plasmid DNA) is also provided and contains homology to the sequences next to the cut site. An alternate technique, known as Receptor-Mediated Ovary Transduction of Cargo (ReMOT Control) (Chaverra-Rodriguez et al., 2018; Wu et al., 2021), enables germline editing by merely injecting into the thorax of adult females (as opposed to embryo-injections) (Jasinskiene et al., 2007; Kistler et al., 2015) (Figure 1.4). ReMOT Control involves a combination that transports the Cas9/gRNA complex from the female haemolymph (insect blood) to the developing oocytes (eggs) by means of an endosomal escape reagent and a modified Cas9 protein with a fused peptide (P2C), that facilitates Cas9 RNP transduction from the female haemolymph to growing mosquito eggs. The offspring as a result undergo heritable gene editing. ReMOT Control has been employed to create heritable NHEJ mutations in a number of mosquito species, but it has not yet been optimized to allow for HDR DNA insertion (Chaverra-Rodriguez et al., 2018; Wu et al., 2021). Both embryonic microinjection and ReMOT Control technique have been successfully used in several insects including *Ae. aegypti* (Chaverra-Rodriguez et al., 2018; Dong et al., 2015; McKenzie et al., 2018; Sun et al., 2022). Embryonic microinjection method has been used repeatedly in the past decade in the mosquito *Ae. aegypti* (Bui et al., 2023; Dong et al., 2015; Kistler et al., 2015; McKenzie et al., 2018; Sun et al., 2022); however, the ReMOT Control technique, despite being easier and cheaper, has only been utilized recently and is less optimized.

The utilization of CRISPR/Cas9 in the mosquito species *Ae. aegypti* has yielded significant advancements. Kistler et al. used CRISPR/Cas9 to produce different mutations in *Ae. aegypti* utilising distinct repair pathways (Kistler et al., 2015). Their research offered a thorough examination of the potential of CRISPR/Cas9 in *Ae. aegypti*, opening up hitherto inaccessible opportunities for genetic alteration in non-model organisms (Kistler et al., 2015). Using CRISPR/Cas9, several knockout lines were developed in the mosquito *Ae. aegypti* that same year.

For example, CRISPR/Cas9 was used to successfully introduce mutations into *Ae. aegypti* for the first time (Dong et al., 2015). By deleting the *Nix* gene, Hall et al. (2015) reported a unique vector mosquito control technique that caused female mosquitoes to become harmless male mosquitoes (Hall et al., 2015). Using a transient embryo test, Basu et al. (2015) increased the effectiveness of CRISPR/Cas9 gene editing in *Ae. aegypti* by identifying highly effective single-guide RNAs (sgRNAs). As shown by plasmid-based reporters, microinjection of double-stranded RNAs targeting *ku70* or *lig4*, both crucial elements of the end-joining response, improved recombination-based repair in early embryos (Basu et al., 2015). In 2016, Zhang et al. created a miR-309 knockout line in *Ae. aegypti*, which caused the mosquitoes to have severe ovarian abnormalities (Zhang et al., 2016). These studies illustrate several uses of CRISPR/Cas9 in *Ae. aegypti*, from creating mutations and knockout lines to creating novel methods for controlling vector mosquitoes and examining particular gene functions.

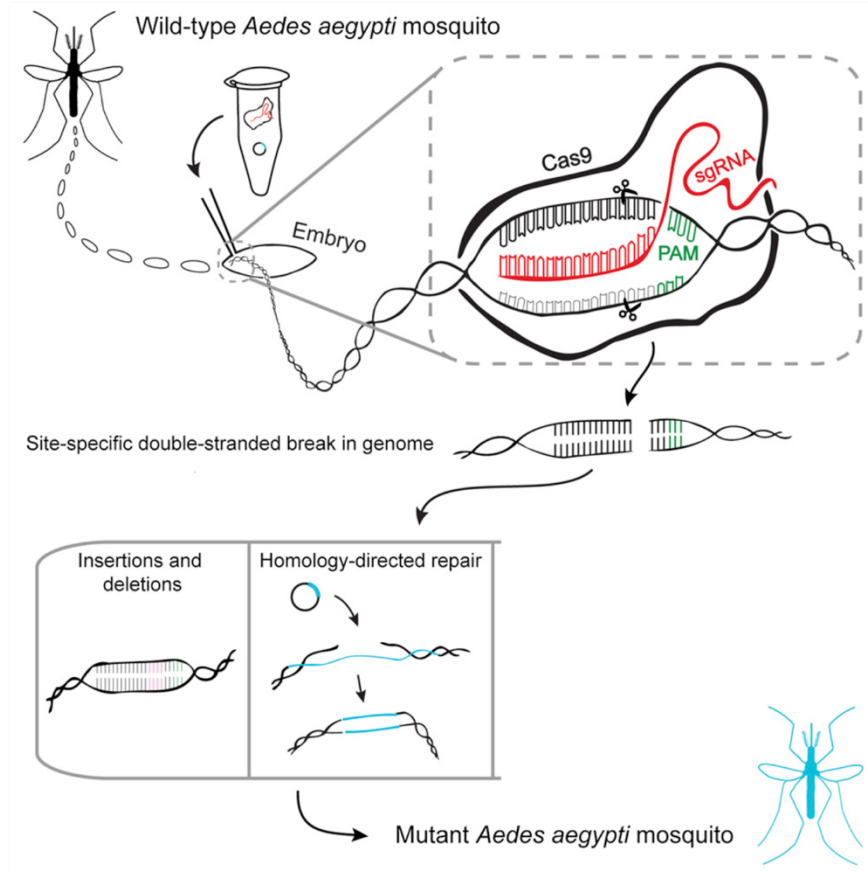


Figure 1.3: CRISPR/Cas9 gene editing technique and delivery strategy utilising embryonic microinjection. A double stranded DNA break caused by CRISPR/Cas9 can be fixed in one of two ways: either error-prone non homologous end joining (NHEJ), which introduces imprecise mutations into the target location, or homology directed repair (HDR), which allows for the exact insertion of targeted DNA segments. Figure adapted from (Kistler et al., 2015).

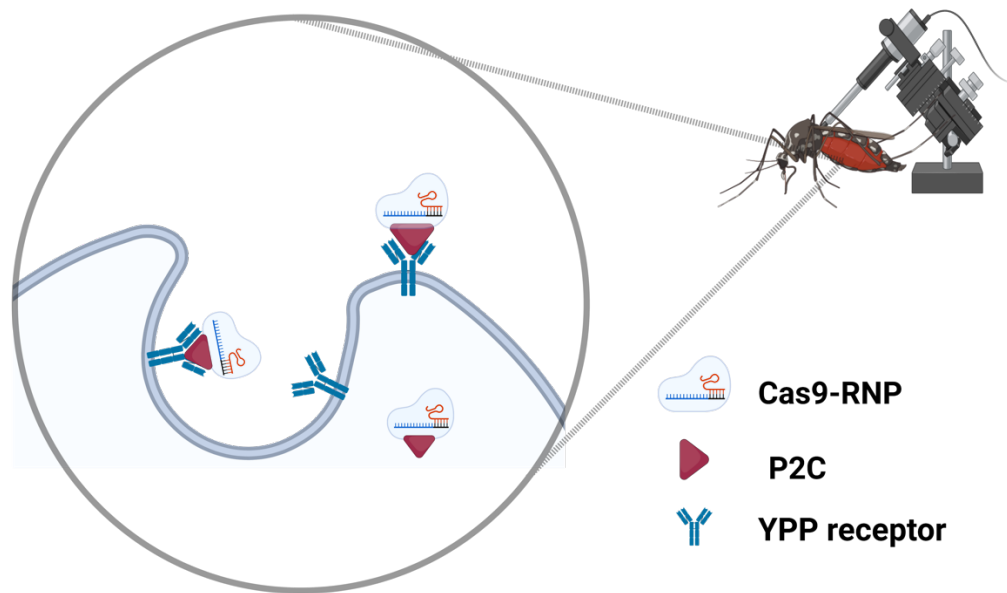


Figure 1.4: CRISPR/Cas9 gene editing technique and delivery strategy utilising ReMOT control. In this technique, when injected into the haemolymph of vitellogenic females, ligand produced from arthropod yolk protein precursors (YPPs) are fused or coupled to molecular cargo such as the Cas9 ribonucleoprotein (RNP) complex and are transported into the oocyte at levels required to induce genome editing in the embryo. The transport of the Cas9 ribonucleoprotein (RNP) from the female haemolymph to mosquito oocyte development is facilitated by the peptide (P2C). In this method, yolk protein receptors are expressed on the membrane of developing oocytes within the ovaries after a female mosquito has engorged on a blood meal. Figure was created using BioRender.com.

1.6. Research objectives and hypotheses

According to previous reports, the saliva of *Ae. aegypti* mosquitoes contains a peptide with the pharmacological characteristics of a tachykinin that is 1410 Da in size. It was discovered that this vasodilator is made up of two peptides: sialokinin I, which has the amino acid sequence Asn-Thr-Gly-Asp-Lys-Phe-Tyr-Gly-Leu-Met-NH₂, and sialokinin II, which is the same as sialokinin I with the exception of an Asp in position 1. Both peptides have the same level of activity as substance P of the mammalian tachykinin when tested on the guinea pig ileum (Champagne and Ribeiro, 1994). Sialokinin I and II, which are tachykinins of the vertebrate type, were identified from salivary glands, although it is unclear if similar peptides also occur in the neural systems of insects. On the other hand, the salivary glands do not appear to have the invertebrate form of TKRPs (Nässel, 1999), which is the focus of my research.

In 2007, Nene et al. conducted whole genome sequencing studies on the mosquito species *Ae. aegypti*. This dataset revealed the presence of four distinct transcripts of the tachykinin (*tk*) gene that produce five TKRPs (Nene et al., 2007). Earlier studies had localized tachykinin immunoreactive endocrine cells in the midgut of adult female *Ae. aegypti* where endocrine cells were found in the anterior midgut as well as the very anterior (frontal) and posterior (caudal) regions of the posterior midgut (Veenstra and Costes, 1999). The midgut is the primary site of digestion and nutrient absorption in insects (Veenstra and Costes, 1999), suggesting mosquito TKRPs may function in roles related to these processes.

However, despite these findings, the functions of TKRPs in *Ae. aegypti* mosquitoes remain unknown. In the fruit fly *D. melanogaster*, which is a well-studied model organism, TKRPs have been extensively investigated. Fruit fly TKRPs are involved in diverse physiological processes such as regulation of feeding behavior, modulation of gut motility, regulation of water balance,

control of reproductive behaviors, and modulation of the immune response (Nässel et al., 2019). It is possible that TKRPs in *Ae. aegypti* mosquitoes might have similar functions to those established in fruit flies, considering their close evolutionary relationship and the overall conservation of tachykinin signaling across Bilateria. Therefore, since functions of TKRPs have not been extensively investigated in the *Ae. aegypti* mosquito, the first objective of this thesis was to confirm the localization of TKRPs in the midgut of the mosquito *Ae. aegypti* and examine whether immunoreactivity of these cells changes under different conditions including development, age and feeding status (blood and sugar). Based on expression profiles of TKRPs in *D. melanogaster* (Winther et al., 2006), it was hypothesized that **TKRPs expression would vary over development and reach the greatest abundance of immunoreactivity in the adult stage.** To test this hypothesis, I will examine TKRP immunoreactivity in the midgut of late larval stages and in both male and female adult mosquitoes. Moreover, based on transcriptomic data available on *Aedes atlas* (Hixson et al., 2022) indicating no change *tk* abundance following blood feeding, it was hypothesized that **TKRP immunoreactivity in the midgut would not change after blood feeding.** To test this hypothesis, I will examine TKRP immunoreactivity in the midgut after allowing females to feed on vertebrate blood. Finally, based on the function of TKRPs in the digestive tract of *D. melanogaster* (Nässel et al., 2019), it was hypothesized that **TKRP immunoreactivity would vary based on sugar feeding status with lowest expression expected in starved mosquitoes.** To test this hypothesis, I will examine TKRP immunoreactivity in the midgut of mosquitoes fed *ad libitum* on sucrose solution as well as in starved mosquitoes.

The second objective of this thesis was to generate *tk* knockout *Ae. aegypti* mosquitoes using CRISPR/Cas9 system (Chaverra-Rodriguez et al., 2018; Kistler et al., 2015). Based on the previous CRISPR/Cas9 studies in the mosquito *Ae. aegypti* (Kistler et al., 2015), it was

hypothesized that ***tk* knock-outs would exhibit changes in their gene sequence as well as the expression of tachykinin peptides.** To test this hypothesis, I will monitor the immunoreactivity of the tachykinin peptides through immunohistochemistry in *tk* mutant mosquitoes comparing to wild-type. Moreover, to validate the mutations, I will perform Sanger sequencing on *tk* gene comparing to the wild-type mosquito gene sequence.

2. Materials & Methods

2.1. Mosquitoes

Eggs of *Ae. aegypti* (Liverpool strain) were collected from a laboratory colony and hatched in double-distilled water in an environmental chamber (26°C, 12:12 hour light:dark cycle). Larvae were fed daily with several drops of a solution comprised of 2% (w/v) Argentine beef liver powder and 2% (w/v) brewer's yeast. Adult female *Ae. aegypti* were routinely fed on sheep blood in Alsever's solution (Cedarlane Laboratories, Burlington, ON) using an artificial feeding system. In this system, after spinning down the blood for 5 minutes at 5000 rpm, the majority of plasma was removed, and the concentrated red blood cells were placed into a beaker and covered with parafilm. The beaker containing blood was placed in warm water (~ 40°C) prior to blood feeding mosquitoes. All adult mosquitoes were fed 10% sucrose solution *ad libitum* in a microcentrifuge tube fitted with a cotton ball.

2.2. Immunohistochemistry

Mosquitoes were briefly anesthetized with CO₂ and dissected at room temperature (RT) in nuclease-free Dulbecco's phosphate-buffered saline (DPBS; Wisent Inc., St. Bruno, QC). Whole gut tissues from 4th instar larvae as well as adult male and female mosquitoes were then transferred to 4% paraformaldehyde fixative for 1 hour at RT, rinsed once with DPBS and then incubated for 1 hour at RT to permeabilize the tissues with 4% Triton X-100, 10% normal sheep serum (NSS) (v/v) and 2% BSA (w/v) prepared in DPBS. Subsequently, after three 10-min washes with DPBS, whole gut tissues were then incubated for 48 h at 4 °C with gentle agitation in primary antibody solution (prepared in advance) containing *Leucophaea* Tachykinin-Related Peptide (LemTRP-1, APSGFLGVRa) antiserum provided by Dr Dick Nässel, Stockholm University (Nässel and

Winther, 2002) and diluted 1:2000 in 0.4% Triton X-100, 2% NSS (v/v) and 2% BSA (w/v) in DPBS. Control experiments were performed by omitting the primary antibody. Both experimental and control primary antibody solutions were prepared one day in advance and incubated at 4 °C overnight prior to their application to adult mosquito tissue/organ samples. Following primary antibody treatments, tissues were washed three times for 10 min each with DPBS, samples were then incubated overnight at 4 °C with goat anti-rabbit Alexa 568 (Life Technologies, Burlington, ON) secondary antibody (1:500) solutions containing 10% NSS made up in DPBS. Tissues were mounted on cover slips with mounting media containing 4ug/mL 4',6-Diamidino-2-phenylindole dihydrochloride (DAPI) (Molecular Probes, Eugene, OR) and 50% glycerol in DPBS to visualize cell nuclei and analyzed using an EVOS fluorescence microscope (Life Technologies, Burlington, ON).

2.3. Starvation assay

Starved male and female mosquitoes of between 0 to 6 hours old were isolated and divided randomly into 2 jars with different diet conditions to examine impacts of starvation stress on the TKRP immunoreactivity. Test conditions included 10% sugar fed for 72 hours and starved for 72 hours. Mosquitoes were collected and midguts were dissected for whole mount immunohistochemistry as described above.

2.4. Blood feeding assay

Adult female mosquitoes were raised under typical rearing conditions with males, following the previously mentioned protocol, until they were four days old and had not engorged a blood meal. Then, using an artificial feeding membrane as previously mentioned, they were given pre-

warmed (~37°C) sheep blood (Cedarlane Laboratories, Burlington, ON) for 20 minutes. Females that had completed blood feeding, identifiable by the red colour of their enlarged abdomen, were separated and housed in small cages containing 10% sucrose solution. At 24 hours following blood feeding, these mosquitoes were collected, and their midguts were dissected for whole mount immunohistochemistry as described above.

2.5. Transforming plasmids into bacteria and protein expression induction

pET28a-P2C-Cas9 and pET28a-P2C-EGFP-Cas9 plasmid constructs were generously provided by Prof. Jason Rasgon at Pennsylvania State University and described previously (Chaverra-Rodriguez et al., 2018). Plasmids were transformed into *E. coli* BL21 strain and *E. coli* DH 5alpha (positive control), and grown overnight at 37°C on Luria Broth (LB) agar plates with 25 µg/mL kanamycin antibiotic. Transformation of bacteria was verified by selective growth on kanamycin plates. Plasmids miniprep was done using Monarch® Plasmid Miniprep Kit (New England Biolabs, Whitby, On). To confirm the presence of the correct constructs, these plasmid miniprep samples were sent for Sanger sequencing (The Centre for Applied Genomics, Sick Kids, Toronto, ON).

Recombinant protein induction method was initially adapted from Chaverra-Rodriguez et al. (2018) where BL21 colonies were inoculated overnight at 30°C in 8 mL LB agar media supplemented with 25 µg/mL kanamycin antibiotic. The next day, each preculture was added to 1L LB media containing 25 µg/mL kanamycin and incubated at 37°C for 4 hours until the culture reached an optical density (OD) = 0.6 at a wavelength of 595 nm, when Isopropyl β-D-1-thiogalactopyranoside (IPTG) was added. At this point, different concentrations of IPTG were tried

each time including: 50 μM , 100 μM , 250 μM , 500 μM to optimize recombinant protein expression. Induced cultures were incubated over either 1 night and 2 nights.

2.6. Protein purification

After induction was complete, bacterial cultures were centrifuged at 5000 rpm for 10 minutes, and the bacterial pellet was resuspended in lysis buffer (NEBExpress) and placed at -80°C for 20 minutes. Samples were then thoroughly thawed and sonicated using methods described by Chaverra-Rodriguez et al. (2018). Cells were spun down at $12000 \times g$ for 15 minutes and the supernatants were used for protein purification using NEBExpress[®] Ni spin columns kit, and NEBExpress[®] Ni-NTA Magnetic Beads. Eluted proteins were dialyzed in a centrifugal protein concentrator (30k MWCO). Concentrator tubes were sterilized with 70% ethanol and centrifuged for 10 minutes at 5000 rpm. This step was repeated with sterilized dialysis buffer (50 mM Tris-HCl pH 8.0, 300 mM KCl, 0.1 mM EDTA, 0.5 mM PMSF). Samples were diluted (1:10) in dialysis buffer and added to concentrator tubes and centrifuged for 5 minutes at 5000 rpm. Centrifugation was repeated 3 times with 10 mL dialysis buffer until 1mL of sample remained.

2.7. Coomassie blue staining and immunoblot assay

Purified proteins were loaded on sodium dodecyl sulfate-polyacrylamide gel electrophoresis (SDS-PAGE) to test the purity and visualize by Coomassie blue staining. Prior to western blot assay, samples were quantified using Bradford assay and 100 μg of each protein sample was resolved on 8% SDS-polyacrylamide gels at 100V for 140 – 150 minutes. Proteins were then transferred to polyvinylidene difluoride (PVDF) membrane at 100V for 150 minutes. After an hour of blocking on PBSTB, membranes were incubated overnight at 4°C in PBSTB containing mouse

monoclonal anti-His (1:1000), or Cas9 antibody (1:1000). The next day, membranes were washed three times with PBSTB and incubated in PBSTB supplemented with anti-mouse HRP conjugated secondary antibody (1:1000) at room temperature for 1 hour and washed again three times with PBST. Protein bands were visualized using a ChemiDoc MP Imaging System (Bio-Rad Laboratories, Mississauga, ON) and molecular weight analysis was performed using Image Lab 5.0 software (Bio-Rad Laboratories, Mississauga, ON) after incubating with ECL substrate for 5 minutes.

2.8. Female injection and dissection

Adult females were blood fed 24 hours before injection, immobilized at 4 °C for 15 minutes and kept on ice during injection (Chaverra-Rodriguez et al., 2018). Injections were performed intrathoracically using a Nanoject III Programmable Nanoliter Injector (Drummond Scientific, Broomall, PA, USA) with 200 nL of P2C-EGFP-Cas9, or the dialysis buffer alone, injected into each female. Different times (18 hrs and 24 hrs) after injection were adapted for dissections and confirmation of EGFP uptake into the ovary. Three groups of non-injected, saline (dialysis buffer) injected, and P2C-EGFP-Cas9 (1433.02 µg/mL) injected females ovaries were dissected, fixed in 4% paraformaldehyde for 1 hour, and subsequently washed 3 times with DPBS. Tissues were transferred onto slides in mounting media containing 4µg/mL 4',6-Diamidino-2-phenylindole dihydrochloride (DAPI) (Molecular Probes, Eugene, OR), 50% glycerol in DPBS, covered with coverslip and imaged on an EVOS FL Auto Live-Cell Imaging System (Life Technologies, Burlington, ON).

2.9. sgRNA design, synthesis, and purification

Six sgRNA oligo templates and two pairs of primers (Table 2.1; Figure 2.1) were designed according to protocols described earlier (Kistler et al., 2015; McKenzie et al., 2018) using CHOPCHOP and CRISPR Guide Express tools targeting the *Ae. aegypti tk* gene. sgRNAs were ranked according to their isoform coverage, efficiency score, off target region, machine learning score based on flies and distance to the start codon. sgRNA were synthesized using EnGen[®] sgRNA Synthesis Kit, *S. pyogenes* (New England Biolabs, Whitby, On) and subsequently purified using Monarch[®] RNA Cleanup Kit (50 µg) (New England Biolabs, Whitby, On).

Table 2.1: sgRNA oligos and genome screening primers. a: sgRNA oligos; bolded parts are 20bp target-specific DNA sequence. Six sgRNAs and two pairs of primers were designed according to the protocol described by Kistler et al. (2015) using CHOPCHOP and CRISPR Guide Express tools (Kistler et al., 2015; McKenzie et al., 2018) targeting the *Ae. aegypti tk* gene. The PAM (NGG) sequence is required for Cas9 recognition target sequence and is not part of the sgRNA sequence and is removed here. The 5' end of the oligo contains T7 promoter sequence (shown in blue). One "G" was added to 5' end of psgRNA/sgRNA sequences that do not begin with a "G" in order to facilitate transcription (Added "G"s were underlined). The 3' end of the oligo includes the 14 nucleotides overlap sequence (shown in red). b: genome sequencing primers.

	Oligos
sgRNA 1	5'- TTCTAATACGACTCACTATA <u>G</u> TTGCCGCTACTGGACACAGATTTTAGAG CTAGA-3'
sgRNA 2	5'- TTCTAATACGACTCACTATA <u>G</u> GACACAGATGGCACATCGATTTTAGAG CTAGA-3'
sgRNA 3	5'- TTCTAATACGACTCACTATA <u>G</u> GTACCCACCGATAACGATGATTTTAGAG CTAGA-3'
sgRNA 4	5'- TTCTAATACGACTCACTATA <u>G</u> CCTTAAGATTGTATCCTAAGTTTAGAG CTAGA-3'
sgRNA 5	5'- TTCTAATACGACTCACTATA <u>G</u> TATCCTAAGCGGGCTCCTTCTTTAGAG CTAGA-3'
sgRNA 6	5'- TTCTAATACGACTCACTATA <u>G</u> TCCGGTTTCCTTGGCTTGAGTTTAGAG CTAGA-3'

(a)

Primer name	Primer sequence	Purpose
sgRNA1-3-FOR	GACCATTATTATAGCGAAGGCG	Used for screening mosquitoes injected with sgRNA1, 2 and 3
sgRNA1-3-REV	TAATGGAATTCATCATCAAGCG	
sgRNA4-6-FOR	CTCAACACACATAGGATGTCCG	Used for screening mosquitoes injected with sgRNA4, 5 and 6
sgRNA4-6-REV	TTCAAGCTGGTTTGTGTTATCG	

(b)

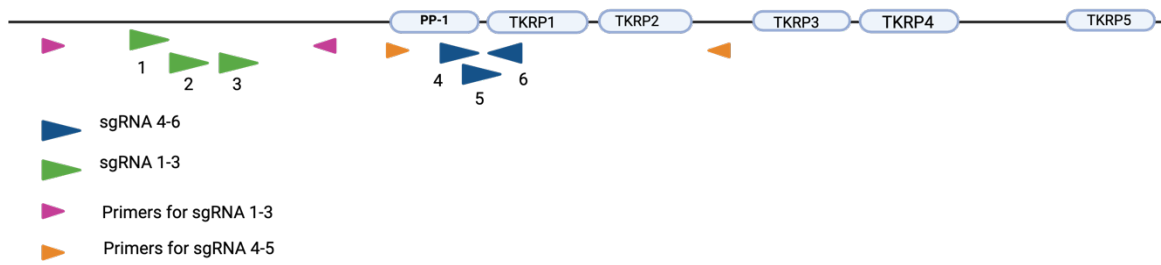


Figure 2.1: Six different sgRNAs and two primer sets. Five transcripts of TKRPs in the mosquito *Ae. aegypti*.

2.10. Preparing the injection mix

For ReMOT technique, P2C-Cas9, sgRNAs and endosomal escape reagent (chloroquine) with the concentrations of 4264.58 ng/ μ L, >1000 ng/ μ L and between 0.5 and 2mM were prepared, respectively, as described previously (Chaverra-Rodriguez et al., 2018). The injection mix was prepared fresh before each injection.

For embryonic injection technique, Cas9 protein (*Streptococcus pyogenes*, recombinant, expressed in *E. coli*, 1X NLS, Sigma-Aldrich) and sgRNAs mix was prepared fresh before each injection with the concentrations of 300 ng/ μ L and 80 ng/ μ L, respectively.

2.11. Embryonic microinjection

In the first step, a cage containing male and female mosquitoes was prepared. After 4-5 days of unrestricted mating in the cage, females received two days of blood feeding using either human blood (from the arm of a volunteer) or sheep's blood (Cedarlane Laboratories, Burlington, ON). There were no other sources of moisture in the cage other than the sugar feeder since adults could prematurely deposit eggs and hinder the timely oviposition needed for embryo injections. A vial for oviposition was made (Figure 2.2.a) on the day of embryonic microinjections (72 hours after the second day of blood feeding), and about 6-7 females were added from the cage. The vial was placed inside a cardboard box providing a low light environment, which was then placed in an incubator set to 27°C for 40–50 minutes to promote oviposition.

Using a fine-tip paintbrush, individual eggs were aligned side by side on ddH₂O wetted filter paper (enough moisture to keep the eggs moist without a meniscus forming). For microinjection, the narrow posterior poles of the embryos were all pointed in the same direction (Figure 2.2a). After aligning approximately 50 embryos that were white to light grey in coloration, the water

from the wet filter paper were absorbed to soak up residual moisture to help the embryos stick better to the double-sided tape used in the next step. To transfer embryos onto a glass slide for microinjection, a piece of double-sided sticky tape was adhered to a glass slide, and a piece of Tegaderm was placed over top and the slide was gently pressed against the surface of the aligned embryos. The embryos were immediately covered with water-saturated halocarbon oil, consisting of a mixture of 9 mL halocarbon oil 700, 1 mL halocarbon oil 27, and 20 mL ddH₂O. Quartz needles were used for injection (Figure 2.2.c) which were prepared using a Sutter P2000 electrode puller with the following setting: heat = 750, Fil = 4, Vel = 40, Del = 150, Pul = 165.

When embryos are white/light grey in color (about 40 minutes post-oviposition), the needle was loaded with 2ul of injection mixture using Microloader Tips (Eppendorf Canada Ltd, Mississauga, ON) while avoiding bubble formation, and then mounted on a micromanipulator. The needle tip was carefully inserted into the posterior pole of the embryo and the mixture was injected using an Eppendorf Femtojet 4i with a typical injection pressure (PI) of 30-50 Psi and injection time (TI) of 0.1-0.3 s resulting in the injection of a quantity of about 10% of the volume of the embryo (Figure 2.2.a).

After injection, the slide consisting of injected eggs was placed in ddH₂O for ~ 50 minutes and then the majority of the halocarbon oil was carefully removed by absorbing with a Kimwipe. The slides and eggs were placed in a Petri dish and covered with wet paper towels for 4 days at 27 °C. Four days after injection, injected G0 eggs were hatched in ddH₂O in a vacuum drying oven (27°C, 20 Psi, 1 hour).

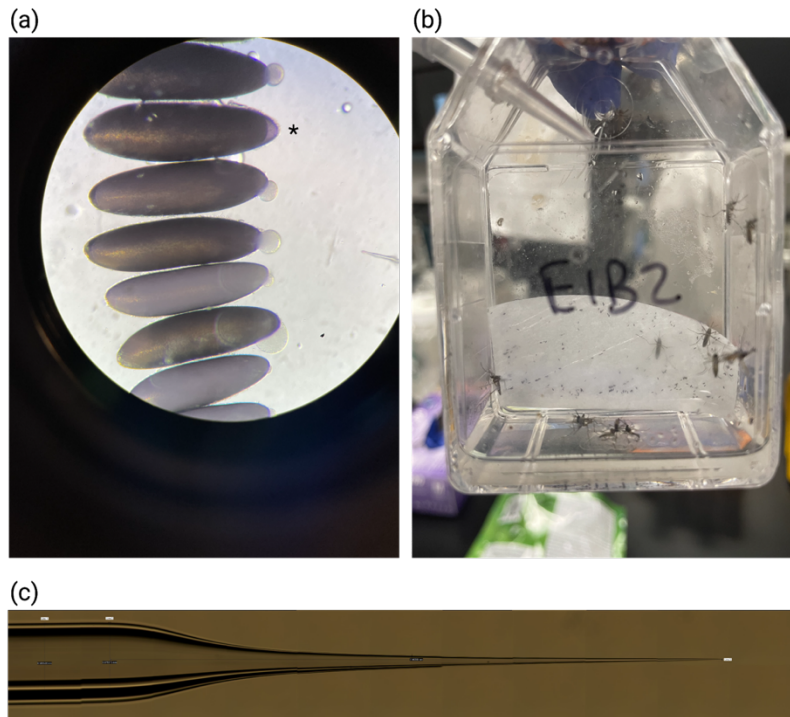


Figure 2.2: Embryonic microinjection. a: Aligned eggs side by side for microinjection. The narrow posterior poles of the embryos are all pointed in the same direction (right side). When embryos are white/light grey in color (about 40 minute post-oviposition, when a pocket is seen on the posterior side of the embryo, shown with *), the needle is loaded with 2ul of injection mixture using Microloader Tips, and then mounted on the micromanipulator. The egg shown with * is before injection and the rest are after injection which the pocket is filled with the injection mix. b: Oviposition chamber with small piece of filter paper for females to lay eggs. c: Quartz needle used for injection.

2.12. HotSHOT genomic DNA extraction and screening by genotyping, heteroduplex mobility and mixed heteroduplex mobility assay

Mosquitoes were isolated at pupal stage in 24 well plates to prevent mating. Adult mosquito half legs were collected after hatching separately in sterile PCR tubes. 50 μ L of a tissue digestion buffer (25mM NaOH and 0.2mM EDTA) (Bhattacharya and Van Meir, 2019) was added to each sample and placed in -80 °C for 15 minutes, and then heated for 30 minutes at 100 °C. Following digestion, 50 μ L of neutralization buffer (40 mM Tris buffer, pH 7.5) was added and isolated DNA samples were stored at -20 °C before subsequent steps. Sample DNAs were amplified using Q5 high-fidelity DNA polymerase (New England Biolabs, Whitby, ON) using the following thermocycler conditions: for sgRNA 1-3 primers (see Table 2.1b), an initial denaturation of 95°C for 30 seconds, 25 cycles of: 98°C denaturation, 61°C annealing, 72°C extension, and final extension: 72°C for 2 minutes; whereas for sgRNA 4-6 primers, all the conditions were same as the previous primers except the annealing temperature was 64°C. High concentration (4%) agarose gels were prepared by dissolving 4g agarose in 100 mL of 1x TAE buffer by heating solution in a microwave. High concentration agarose gels were poured without delay as the gel solidifies quickly. Electrophoresis was performed for 1 hour, and the power supply was set to 100 V with constant voltage. After identification of heteroduplex samples (double bands on agarose gel), in order to identify homozygous mutants, 8 μ L of the sample PCR products of any candidate homozygous mutant samples (single band on agarose gel) were mixed with 8 μ L of the known wild-type PCR template, heated up and cooled down according to the following temperatures: 95°C for 2 min, ramp down to 25°C at 0.1°C per second. These samples were run on a 4% agarose gel for 1 hour with the power supply set to 100 V constant voltage (Figure 2.3).

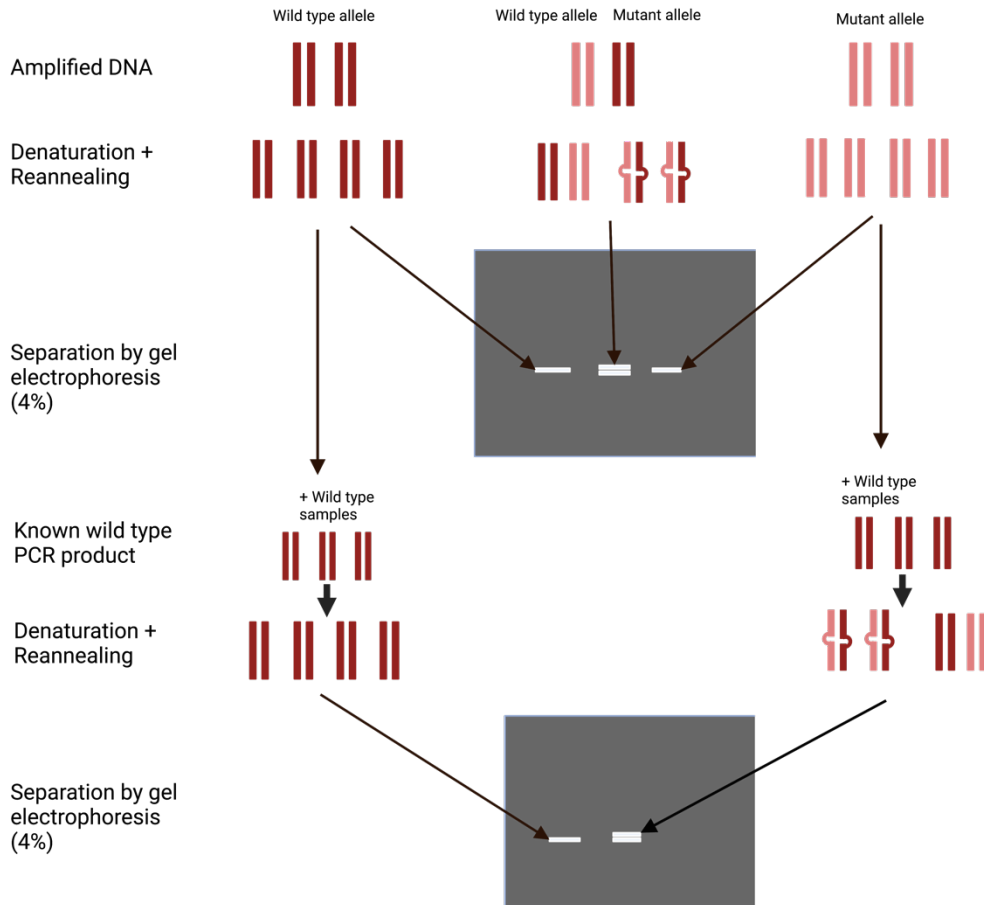


Figure 2.3: Heteroduplex mobility and mixed heteroduplex mobility assay. Amplified DNAs of progeny were run on the 4% agarose gel. Single band samples, representing either homozygous wild type or mutant alleles, each were mixed with a known wild type PCR product at the same proportions and after exposing to a denaturation + reannealing cycle, samples were electrophoresed again. In this second electrophoresis, single bands represent wild type while double heteroduplex bands represent homozygous mutant samples. Figure was created using BioRender.com.

2.13. Colony PCR of pGEM-T Easy vector

Sample DNAs extracted from mosquitoes were amplified by PCR using Q5 high-fidelity DNA polymerase (New England Biolabs, Whitby, ON) with primers designed for those regions (Table 2.1b). After PCR reamplification with Taq DNA polymerase using the same primers, the amplicon was purified using a Monarch PCR purification kit (New England Biolabs, Whitby, ON). Purified products were then ligated to pGEM T Easy vector (Promega, Madison, WI, USA), and then transformed into high efficiency competent *E. coli* cells (New England Biolabs, Whitby, ON). Plasmid DNA miniprep samples were sent for Sanger sequencing (The Centre for Applied Genomics, Sick Kids, Toronto, ON) to confirm the sequence composition of the TK mutants generated.

2.14. Statistical analysis

All cell counting immunohistochemistry images data were analyzed by unpaired t-test. P value < 0.05 was considered significant. Statistical analysis was carried out by GraphPad Prism 9 (GraphPad Software, San Diego, USA).

3. Results

3.1. Immunolocalization of TKRPs in the midgut of the mosquito *Ae. aegypti* over different developmental stages and under various physiological conditions including blood fed, sucrose fed and starvation.

Using a *Leucophaea* Tachykinin-Related Peptide (LemTRP-1) antibody (Nässel and Winther, 2002), immunohistochemistry was performed on the midgut of wild type mosquitoes, one of the main sites of tachykinin production in insects. Localization of TKRP in the midgut of adult mosquito showed TKRP immunoreactivity in the proventriculus, anterior midgut as well as the very anterior (frontal) and posterior (caudal) regions of the posterior midgut (Figure 3.1 and 3.2.b). No differences were observed in the localization of TKRP between male and female adult mosquitoes. To determine whether changes in the distribution of TKRP in the midgut was evident over *Ae. aegypti* developmental stages, late stage larval (4th instar) and different aged adult mosquitoes were examined for tachykinin immunoreactivity. There was no difference observed with respect to TKRP immunoreactivity between 1 day old and 4 day old adult mosquitoes (Figure 3.3, 3.7). Immunohistochemistry in the 4th instar larva localized TKRP in similar areas as adult mosquito (Figure 3.2.a and 3.3); however, it showed reduced TKRP immunoreactivity in the anterior part of midgut compared to one day old adult mosquito midgut (Figures 3.1, 3.2, 3.3 and 3.7). Moreover, immunoreactivity of TKRPs in blood fed and non-blood fed females also showed no significant differences on 5 day old blood fed (24 hours post blood feeding) and non-blood-fed mosquito midgut (Figure 3.5 and 3.7). However, results on 3 days starved and 10% sugar fed mosquitoes showed differences in TKRP immunoreactivity in the anterior midgut of adult 3 day old mosquitoes (Figure 3.6 and 3.7). There is reduced expression in the midgut of starved mosquito *Ae. aegypti* comparing to 10% sugar fed wild type. Cell counting of the immunohistochemistry

anterior midgut images of adult female mosquitoes and 4th instar larvae also supports these observations: 4th instar larval stage showed 69.50 cells (n=6), adult 1 day old 10% sugar fed mosquito showed 107.8 cells (n=16), adult 4 day old 10% sugar fed mosquito showed 109.3 cells (n=21), adult 5 day old blood fed mosquito showed 103.6 cells (n=19), adult 5 day old non blood fed (10% sugar fed) mosquito showed 109 cells (n=24), adult 3 day old 10% sugar fed showed 114.6 cells (n=22), adult 3 day old sugar starved mosquito showed 15.7 cells (n=18). These observed trends in the number of TKRP immunoreactive cells in the anterior midgut was similar in adult male mosquitoes (Figure 3.7).

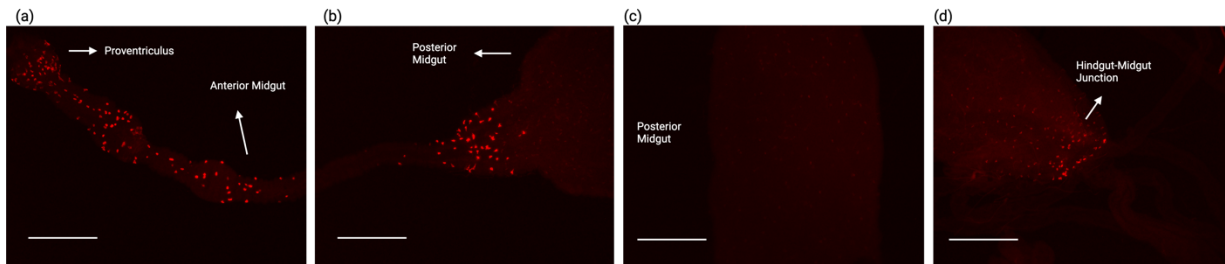


Figure 3.1: Localization of TKRP in the midgut of adult mosquito *Ae. aegypti*. Using a *Leucophaea* Tachykinin-Related Peptide (LemTRP-1) antibody (Nässel and Winther, 2002), immunohistochemistry was performed on the midgut of wild type 1-day-old adult mosquitoes which showed TKRP immunoreactivity in the proventriculus (a), anterior midgut (a) as well as the very anterior (frontal) (b) and posterior (caudal) (d) regions of the posterior midgut. Scale bar: 100 μ m.

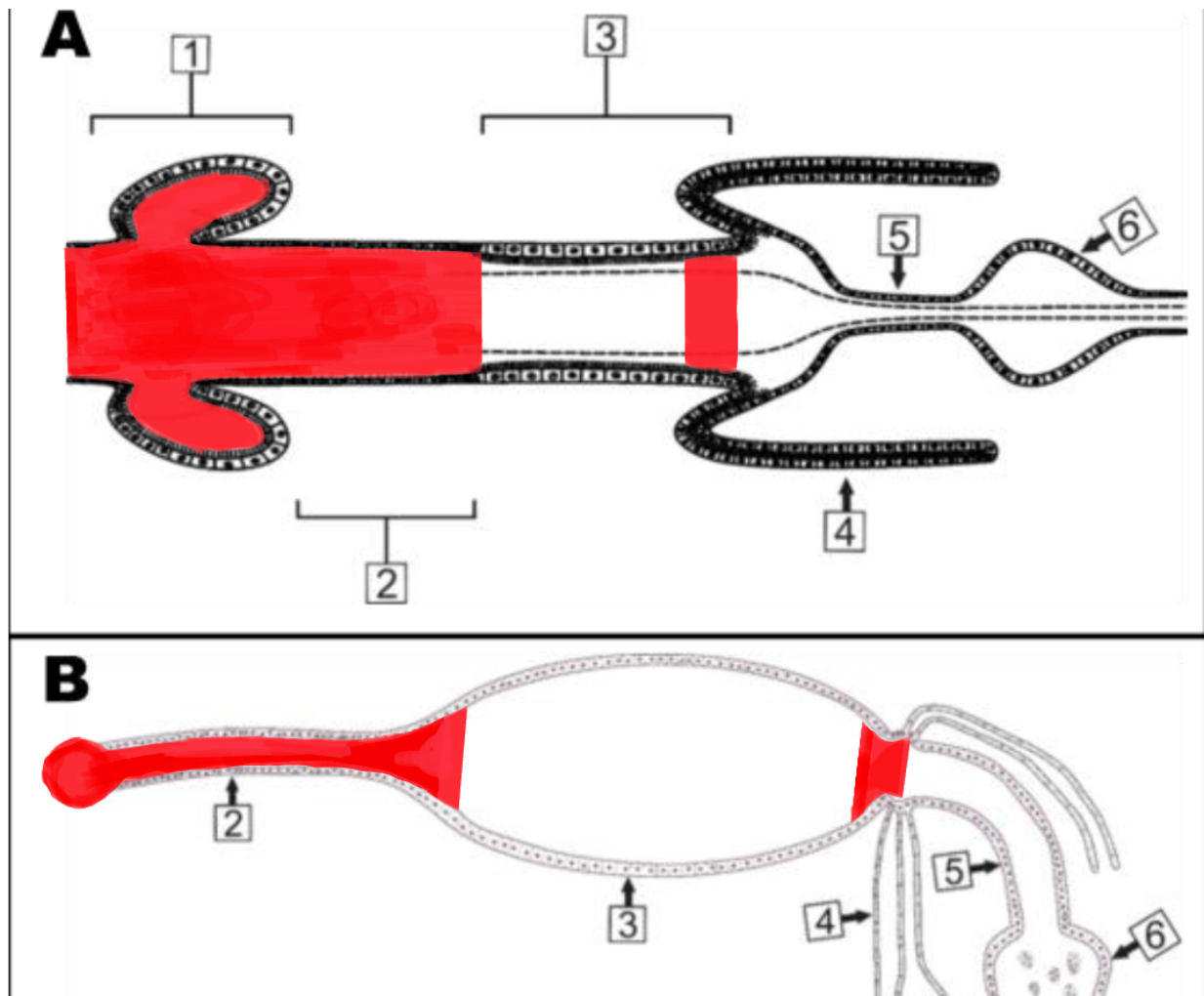


Figure 3.2: Schematic diagram of the midgut of 4th instar larval stage (a) and 1 day old adult (b) *Ae. aegypti* mosquito TKRP immunoreactivity. Immunohistochemistry on larval stage and adult mosquito using a *Leucophaea* Tachykinin-Related Peptide (LemTRP-1) antibody showed TKRP immunoreactivity in the same areas but with reduced immunoreactivity in the 4th instar larvae in anterior midgut as well as the very anterior (frontal) and posterior (caudal) regions of the posterior midgut. 1: gastric caeca, 2: anterior midgut and proventriculus, 3: posterior midgut, 4: Malpighian tubes, 5: ileum, 6: rectum. Figure adapted from (Dixon et al., 2017)

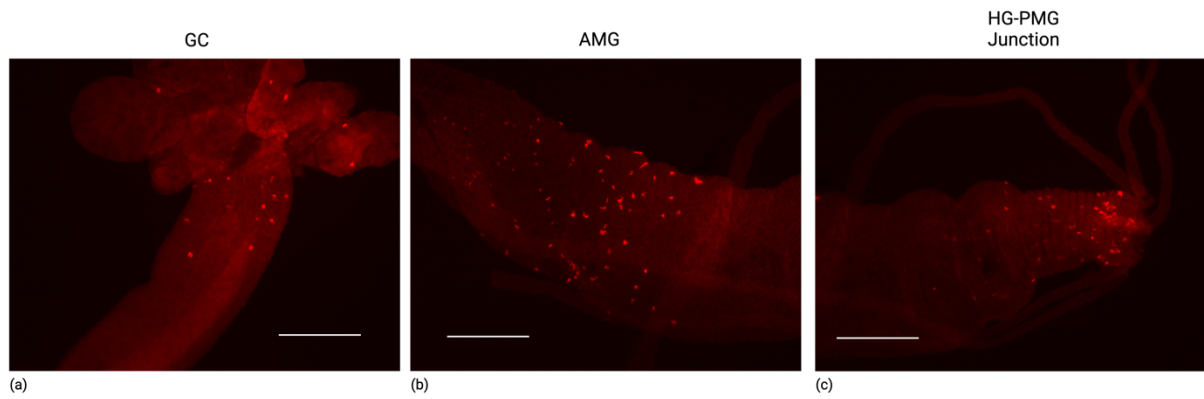


Figure 3.3: Immunohistochemistry on 4th larval stage of the mosquito *Ae. aegypti*. Using a *Leucophaea* Tachykinin-Related Peptide (LemTRP-1) antibody, immunohistochemistry was performed on 4th larval stage of *Ae. aegypti*. TKRP immunoreactivity was observed in gastric caeca (a), anterior midgut (b) and posterior (caudal) (c) region of the posterior midgut. Scale bar: 100 μ m.

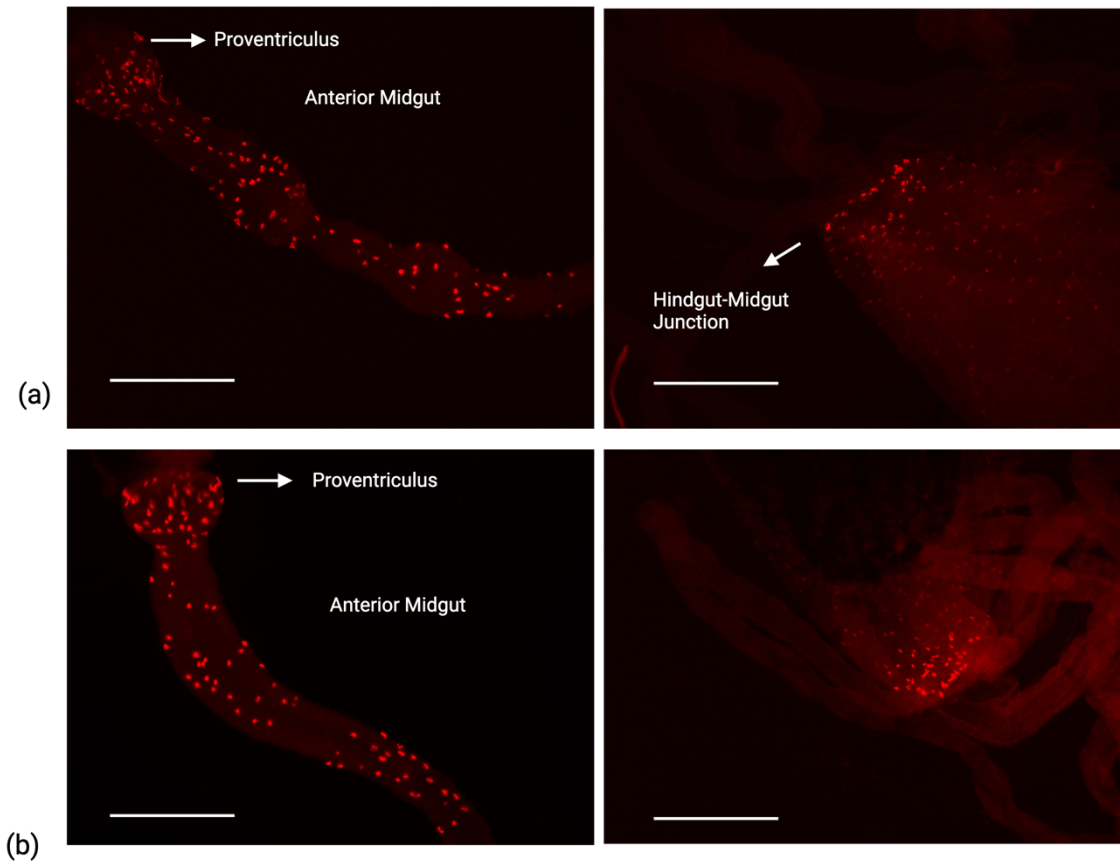


Figure 3.4: Immunohistochemistry on different aged adult mosquitoes. Using a *Leucophaea* Tachykinin-Related Peptide (LemTRP-1) antibody, immunohistochemistry was performed on midgut of wild-type mosquitoes. a: one day old female mosquitoes. b: four-day old female mosquitoes. In both ages, TK immunoreactivity is observed in anterior midgut. Scale bar: 100 μ m.

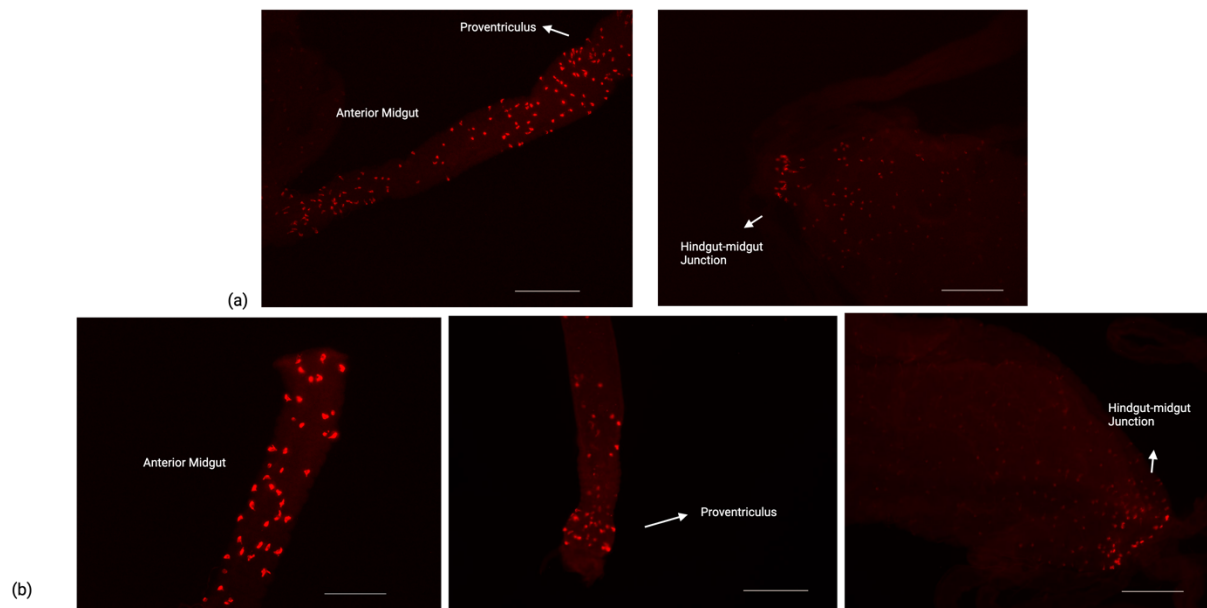


Figure 3.5: Immunohistochemistry on blood fed and non-blood fed adult mosquitoes. A: Midguts from blood fed mosquitoes were dissected 24 hours PBF. B: Midgut from non-blood fed female mosquito. All mosquitoes were at the same age when dissected. Using a *Leucophaea* Tachykinin-Related Peptide (LemTRP-1) antibody, immunohistochemistry was performed on wild-type blood fed and non-blood fed mosquito midguts. Scale bar: 100 μ m.

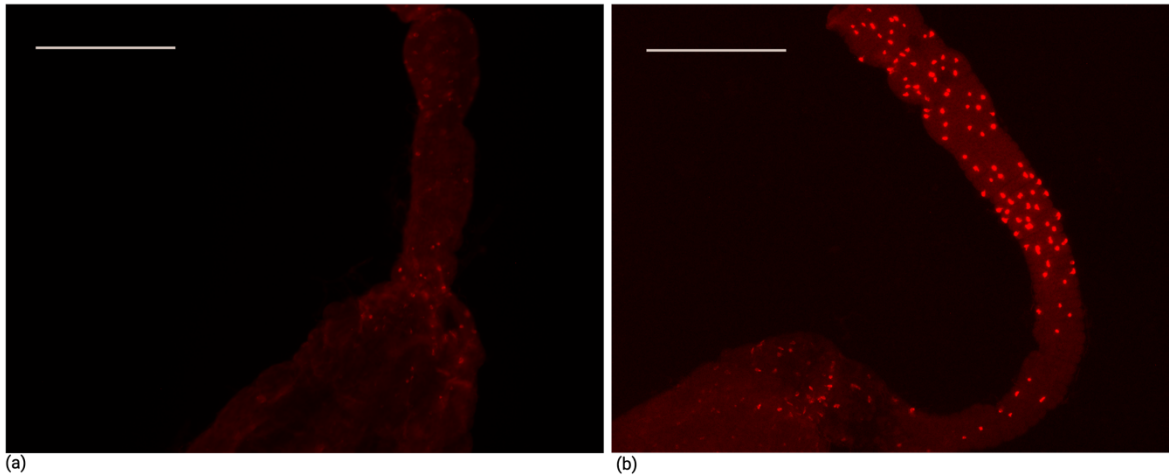


Figure 3.6: Immunohistochemistry on starved (a) and sugar fed (b) mosquitoes. Using a *Leucophaea* Tachykinin-Related Peptide (LemTRP-1) antibody, immunohistochemistry was performed on the midgut of wild-type mosquitoes. All the mosquitoes in this particular experiment were 3 days old. Lowest immunoreactive staining of TKRPs were observed in starved mosquitoes in comparison to strong immunoreactivity observed in sugar fed mosquitoes. Scale bar: 100 μ m.

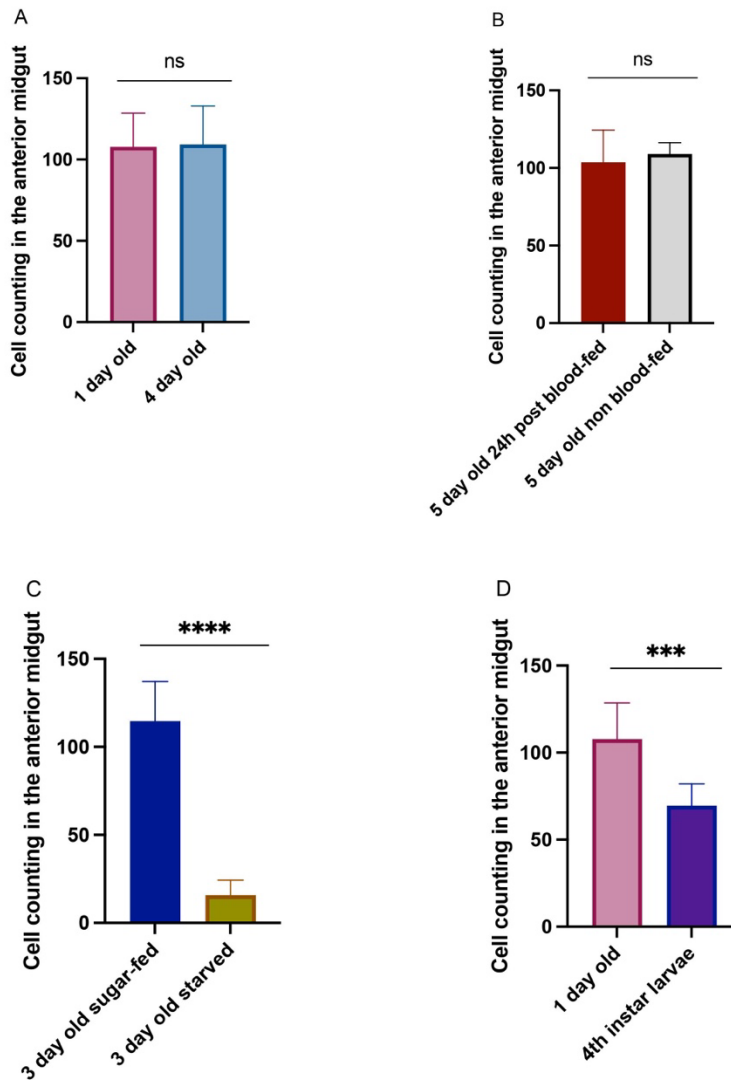


Figure 3.7: Counting of the TKRP immunoreactive cells in the anterior midgut of adult female mosquitoes and 4th instar larvae. No differences in the number of TKRP immunoreactive cells in different aged adult mosquitoes (A) or in female mosquitoes before and after blood feeding (B). Significant differences in TKRP immunoreactivity between adult sugar fed and starved (C) and adult 1 day old and 4th instar larvae (D) were observed. Values are presented as means±SEM and analyzed by unpaired t-test ($P < 0.05$). “****” shows $P \leq 0.001$ and “*****” shows $P \leq 0.0001$.

3.2. Optimization of injection conditions (ReMOT)

The best time to inject females following a blood meal was determined in earlier studies (Chaverra-Rodriguez et al., 2018). As mentioned earlier in this thesis, Chaverra-Rodriguez and colleagues devised a strategy for adult injection of Cas9 into germline tissue for targeted destruction of a visual marker using *Ae. aegypti*. They observed that a 41 amino acid peptide (P2C) generated from DmYP1 was adequate to promote Cas9 uptake into the ovaries, and when combined with an appropriate endosomal escape reagent, the Cas9 RNP precisely targeted the *Ae. aegypti* gene of interest in a heritable and flexible way. The phenotypes observed upon injection of the P2C-Cas9/sgRNA ribonucleoprotein into adult females were likely a reflection of the developmental timing of the mosquito oocyte, implying that the accessibility of chromosomal DNA to the RNP in the oocyte alters during ovarian development. The presence of mutant paternal copies of the gene indicates that the complex is stable and functional during fertilisation, which occurs >24 h after injection (Raminani and Cupp, 1975). Earlier injections (~24 h PBF) resulted in high-efficiency maternal chromosomal editing, but later injections resulted in mosaic G0, showing editing processes in certain somatic cells, and proving that the RNP complex is active in the fertilized embryo (Chaverra-Rodriguez et al., 2018).

In the current study, P2C-EGFP-Cas9 (1433.018 ng/ μ L) construct was injected into females 25 hours PBF following earlier protocols (Chaverra-Rodriguez et al., 2018) and ovaries were dissected 18 and 24 hours post injection. Transduced EGFP was observed in yolk granules throughout oocyte development. EGFP uptake was observed in almost all ovaries dissected 24 hours post injection but in ~ 70 percent of ovaries dissected 18 hours post injection (Figure 3.8), suggesting that the later time post injection is more ideal for dissecting animals.

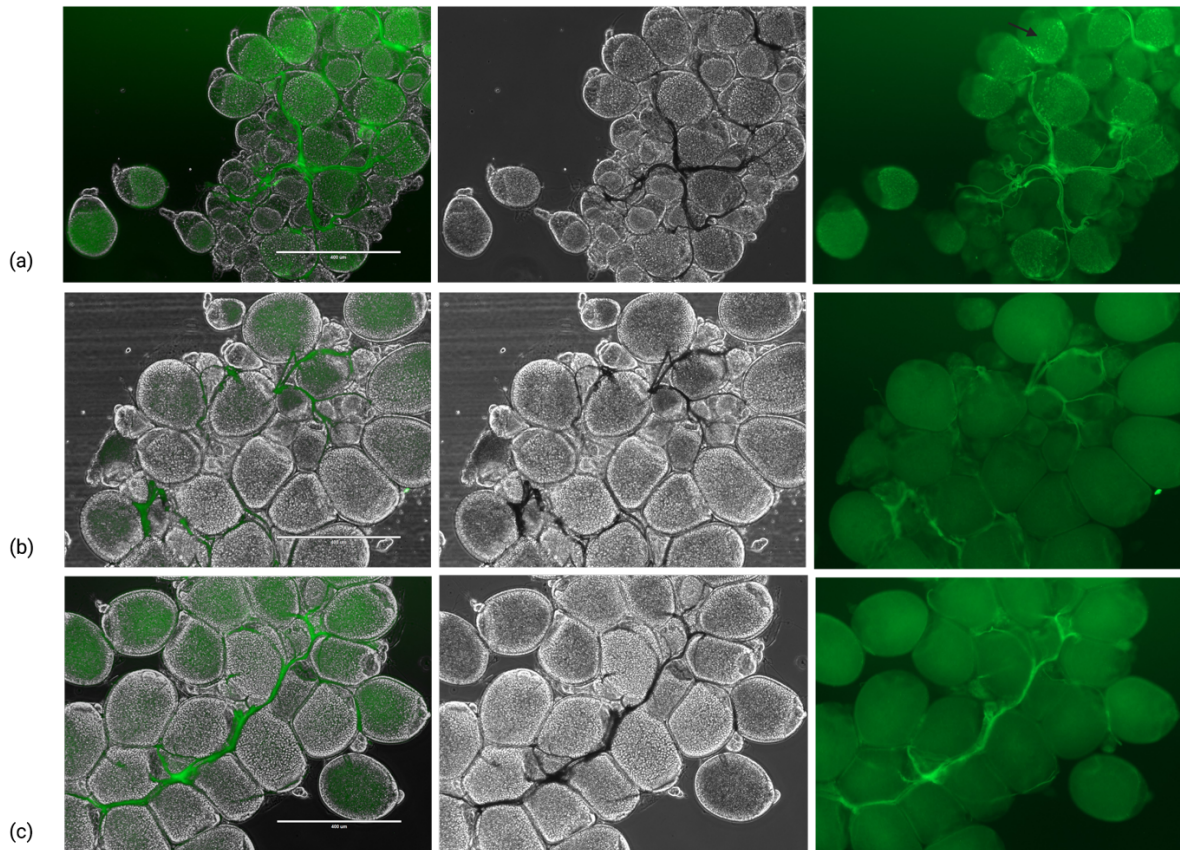


Figure 3.8: P2C-EGFP-Cas9 recombinant protein uptake into ovaries following injection. A: P2C-EGFP-Cas9 injected animals were dissected 24 hours post injection and transduced EGFP is observed in yolk granules (black arrow) (n=11). B and c show the control; saline injected (n=15) and non-injected (n=3) females, respectively. Scale bar: 400 μ m.

3.3. Determining the best sgRNA candidate and embryonic microinjection

Before committing to large-scale injections, we designed multiple sgRNAs (Table 1a) targeting the TK gene to maximize the chance of successful mutagenesis (Kistler et al., 2015). Four different transcripts produce TKRPs (Predel et al., 2010), which mostly yield the same peptides with the exception that two out of the four transcript variants do not encode the fifth peptide. The *tk* gene knockout strategy aimed to disrupt all four transcripts ahead of the first encoded TKRP so that there will be no chance of producing any TKRPs (Figure 2.1).

Six sgRNAs were designed according to the protocol described by (McKenzie et al., 2018) targeting the *Ae. aegypti tk* gene. To find the best candidates, following sgRNA synthesis and purification, they were tested *en masse* in groups of three by embryonic microinjection and progeny were screened as described above (see section 2.8) and sequenced afterward to see where the mutation occurred (Figure 3.9).

From the above sgRNA candidate screen, animals derived from embryos injected by sgRNA 1 and 2 showed different band characteristics in comparison to wild type mosquitoes (control) (Figure 3.2). Those candidate mutant samples were sent for Sanger sequencing (The Centre for Applied Genomics, Sick Kids, Toronto, ON) and double-stranded break induced at the cut site (3 nucleotides upstream of the PAM site) (Figure 3.9) were observed for both sgRNA1 and 2. Accordingly, sgRNA1 and 2 were chosen as the best candidate sgRNAs for the rest of injections.

sgRNA1 was injected into 80 eggs, in which 28 eggs survived and hatched to adult mosquitoes. After screening with PCR amplification of those 28 mosquitoes, 6 of them were chosen and outcrossed to wildtype virgin mosquitoes (Table 3.1). G1 eggs were screened accordingly, and double bands were observed on 4% agarose gel which means the individual has inherited two different alleles for the *tk* gene and is heterozygous (Figure 3.10). Three generations

(G0, G1 and G2) were outcrossed with wild type mosquitoes to achieve a steady tachykinin mutant line. G3 heterozygous mutated animals were chosen to mate together to achieve homozygous *tk* mutant mosquitoes.

Homozygous wild-type or mutant alleles produce only one band on the 4% agarose gel. To distinguish WT/mutants homozygous PCR products are combined with wild-type control samples in equal proportions, exposed to one denaturation/renaturation cycle, and the products are electrophoresed again. Samples obtained from animals with homozygous mutant alleles now have two bands, whereas those from animals with wild-type alleles only have a single band (Figure 2.3) (Bhattacharya and Van Meir, 2019).

Homozygous mutants were identified on the gel and sent for Sanger sequencing (The Centre for Applied Genomics, Sick Kids, Toronto, ON). The results confirmed genetic modification of the *tk* gene had taken place, with a 6 nucleotide deletion (Figure 3.11), which means there was no change in the reading frame but which led to a truncation of the TKRP prepropeptide by two amino acids. Irrespective of this result, immunohistochemistry was conducted on homozygous *tk* mutant progeny and, as was expected, TKRPs expression was still observed over the midgut of mosquitoes (Figure 3.12).

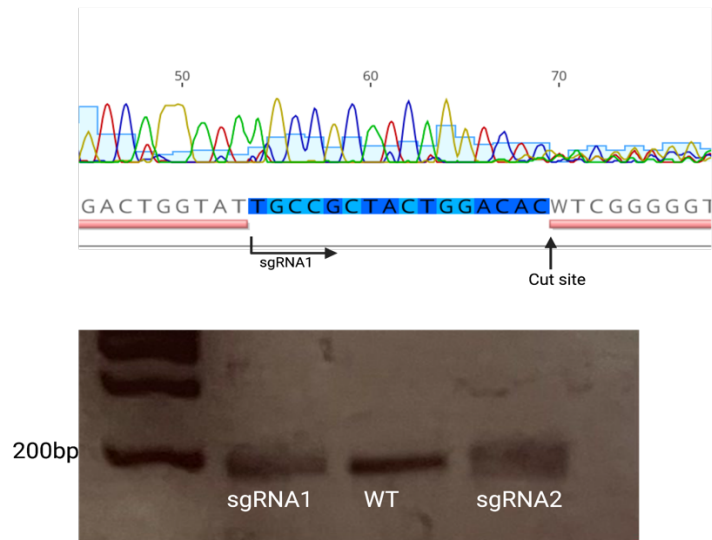


Figure 3.9: Finding the best sgRNA candidate screening. Animals injected by sgRNA1 and 2 (Table 2.1) showed different band characteristics in comparison to wild type mosquito (control). Since in the G0 we do not have heterozygous mutations, double bands will not be seen on 4% agarose gel and mutant animals will show a thicker/faded band (chimeric mutation). Those samples were sent for Sanger sequencing and, double-stranded break induced at the cut site (3 nucleotides upstream of the PAM site).

Table 3.1: Testing out sgRNAs to find the best sgRNA candidate. Survival rate of injecting different sgRNAs to female mosquitoes.

	Survivors/injected eggs
Cas9-sgRNA 1	10/40 (25%)
Cas9-sgRNA 2	6/40 (15%)
Cas9-sgRNA 3	12/30 (40%)
Cas9-sgRNA 4	8/30 (26.6%)
Cas9-sgRNA 5	3/25 (12%)
Cas9-sgRNA 6	5/20 (25%)
Cas9-sgRNA 1, 2, 3	10/33 (30.3%)
Cas9-sgRNA 4, 5, 6	9/37 (24.3%)

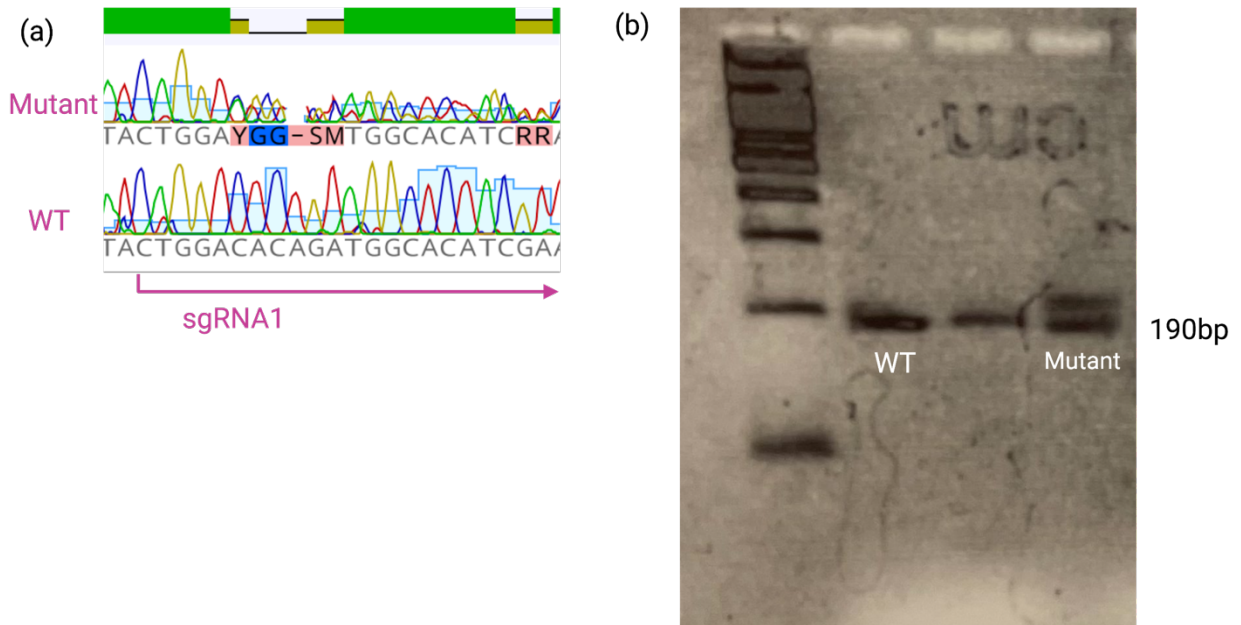


Figure 3.10: G1 sequencing. a: Sanger sequencing of G1 progeny sample compared to wild-type mosquitoes. b: Sample DNA of heterozygous mutant mosquitoes amplified with PCR and appeared as two separate bands on 4% agarose gel (G1 progeny).

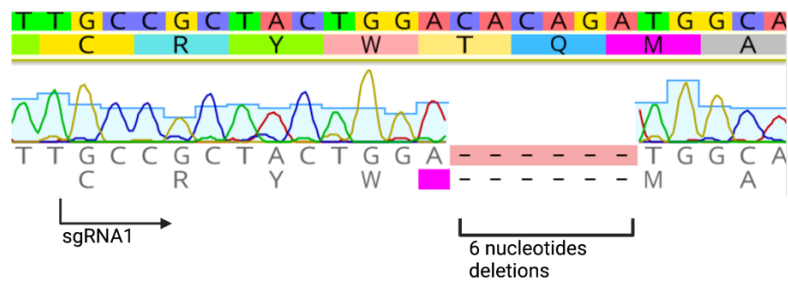


Figure 3.11: Homozygous mutant screening. Sanger sequencing results of homozygous mutant individuals where a 6 nucleotide deletion were observed.

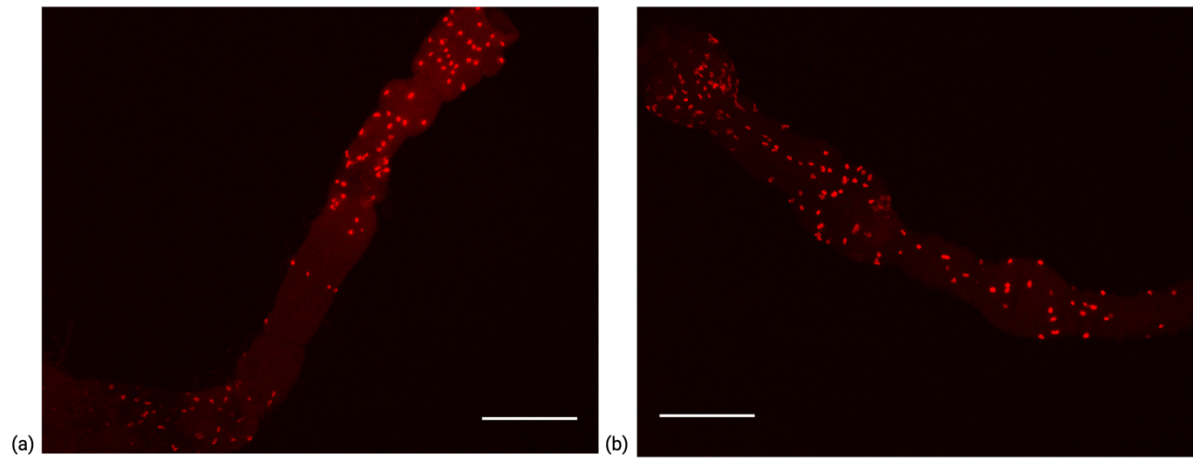


Figure 3.12: Immunohistochemistry on the anterior midgut of homozygous mutants (a) and wildtype (b) adult 1 day old mosquitoes. All mosquitoes were at the same age when dissected. Despite successful modification of the *Ae. aegypti tk* gene, the 6 nucleotide deletion did not impact the detection of TKRP immunoreactivity in endocrine cells within the midgut. Scale bar: 100 μ m.

4. Discussion

The first neuropeptide ever to be isolated from brain tissue was Substance P from mammals, the prototypic TK, which was isolated nearly a century ago (v. Euler and Gaddum, 1931). However, it was not until 1962 that the first invertebrate TK was extracted from the salivary glands of the mollusk *Eledone moschata* called Eledoisin; and it was the first TK to be sequenced (Ersamer and Ersamer, 1962). Four TKs were isolated from the brain and retrocerebral glands of the locust *L. migratoria* many years later (Schoofs et al., 1990a). Today, several TKs (more than 350 sequences) from over 50 insect species including *Ae. aegypti* have been found (Champagne and Ribeiro, 1994; Ribeiro, 1992; Terhzaz et al., 1999). Nonetheless, TKRPs research has remained limited among mosquito species, including *Ae. aegypti*. In this study, using the mosquito *Ae. aegypti*, I tried two methods to knock out *tk* gene including ReMOT Control and embryonic microinjection. Moreover, using a *Leucophaea* Tachykinin-Related Peptide (LemTRP-1) antibody, my research determined the distribution of TKRP immunoreactivity in the midgut of *Ae. aegypti* and compared characteristics of this immunoreactivity in different physiological conditions including blood feeding, developmental stage, and starvation.

4.1 Midgut as one of the major sources of TKRP production in *Ae. aegypti* through development.

Immunohistochemistry results using a *Leucophaea* Tachykinin-Related Peptide (LemTRP-1) antibody (Nässel and Winther, 2002) in *Ae. aegypti* showed TKRP immunoreactivity in the proventriculus, anterior midgut as well as the very anterior (frontal) and posterior (caudal) regions of the posterior midgut of adult females and males (Figure 3.1). These results are consistent with findings involving transcriptomic data that showed that the head and gut are the two major body

parts with prominent TKRP expression in the mosquito *Ae. aegypti* (Hixson et al., 2022), and TKRP immunoreactivity in the midgut are mostly in the anterior midgut and proventriculus (Veenstra and Costes, 1999). Moreover, immunohistology using antiserum to locustatachykinin 2 identified endocrine cells in the anterior midgut, frontal and caudal region of the posterior midgut (Veenstra et al., 1995) in the adult female *Ae. aegypti* mosquito. Furthermore, direct mass spectrometric profiling revealed the existence of TKRPs in the anterior and posterior midgut regions, as well as the dorso-caudal neuropil (DCN) of the terminal ganglia (Predel et al., 2010).

The first hypothesis of this study can be accepted based on the results showing the distribution of TKRP immunoreactivity in 4th instar larval stage were in similar areas as seen in adults, but with reduced TKRP immunoreactive staining intensity (Figure 3.2 and 3.3). This suggests that expression of TKRPs might differ over development with the greatest intensity of immunoreactivity in the midgut of adult stage *Ae. aegypti*. Studies showed a similar expression profile of TKRPs in *D. melanogaster* (Winther et al., 2006) since TKRP immunoreactivity was higher in adults compared to larval stage (Winther et al., 2003). Despite this developmental difference in TKRP immunoreactivity, there was no significant difference observed between one day old and four-day old adult *Ae. aegypti* (Figure 3.4) when animals were reared under standard laboratory conditions with animals provided sucrose solution *ad libitum*.

During the larval stage, the anterior midgut remains an important site for nutrient absorption. It is essential in the processing and digestion of the food consumed by mosquito larvae in their aquatic habitats, which mostly consists of algae, organic waste, and microbes (Raya et al., 2009). However, in the adult stage, the anterior midgut has a somewhat reduced role in digestion of blood compared to the posterior midgut, but has more roles in digestion of sugar derived from imbibed nectar (Cui and Franz, 2020).

4.2. Immunoreactivity distribution of TKRP in different physiological conditions including blood feeding, developmental stage, and starvation.

Hypotheses made in this study regarding TKRP immunoreactive staining intensity in different physiological conditions were all accepted by our results. Specifically, immunoreactivity of TKRPs in the midgut of blood fed and non-blood fed 5-day old females showed no significant differences between blood fed animals (24 hours post blood feeding) and age matched non-blood-fed mosquitoes (Figure 3.5), which is consistent with the transcriptomic data on *AedesAtlas* (Hixson et al., 2022) that showed abundance of the *tk* gene mRNA was similar within the midgut at different time points post blood-feeding. However, results on 3 day old starved and sugar fed mosquitoes revealed dramatic differences in TKRP immunoreactivity in the proventriculus and anterior midgut regions of the gut with lower staining intensity observed in starved mosquitoes (Figure 3.6). These results were also confirmed by counting the number of immunoreactive enteroendocrine cells in the anterior midgut which showed a significant difference in TKRP immunoreactivity between sugar fed and starved mosquitos where the latter showed a dramatic reduction. This is consistent with earlier reported findings of the function of TKRPs in the digestive tract of *D. melanogaster* (Nässel et al., 2019). TKRPs signaling regulates lipid metabolism in the *D. melanogaster* intestine (Song et al., 2014). It has also been shown that TKRPs activity increases when flies are food searching. Immunostaining studies also revealed more TKRPs release in fed flies compared to starved flies (Musso et al., 2021). Quantification of neuropeptides using mass spectrometry after gathering nectar or pollen in honeybees showed that TKRPs are among the three peptides whose levels were most altered by nectar or pollen foraging (Brockmann et al., 2009).

Previous studies showed that the anterior and posterior midguts of the mosquito *Anopheles gambiae* are thought to perform different digestive tasks within the alimentary canal, with the

anterior midgut specialising in nectar digestion and the posterior midgut processing the blood meal (Hecker, 1977). Moreover, Hixson et al. showed that the anterior and posterior midguts in the mosquito *Ae. aegypti*, has roles in protein digestion and sugar digestion/absorption, respectively, based on the enrichment of substrate-specific enzymes for these nutritive compounds (Hixson et al., 2022).

D. melanogaster TK receptor (DTKR) was discovered to be expressed by olfactory sensory neurons of *Drosophila* antennae and TK in subpopulations of antennal lobe local neurons (Ignell et al., 2009). A subsequent investigation revealed more information about the involvement of TK signaling in olfaction and food hunting (Ignell et al., 2009). It was shown that in hungry flies with low circulating insulin-like peptide levels, the DTKR is upregulated in olfactory sensory neurons harboring specific odorant receptors. Upregulation of the inhibitory DTKR in the antennal glomerulus, which conveys food odor aversion, leads to increased TK signaling and thus suppressed depolarization, as well as decreased synaptic activation of antennal lobe projection neurons, leading to increased food attraction in a hungry fly (Ko et al., 2015).

In the mosquito *Ae. aegypti* the anterior midgut has been thought to play little or no part in the process of blood meal digestion because the blood bolus is sealed into the posterior midgut quickly after ingestion by the creation of the peritrophic matrix (Billingsley, 2003). However, it was discovered that the anterior midgut had increased its investment in some categories of digestive enzymes and transporters (e.g. sphingomyelinases, sterol transporters, amylases/maltases, glucosidases, as well as its overall transcriptional yield) late in the blood meal response (24 hr). While the anterior midgut's proportionate production falls in comparison to the posterior midgut, it still contributes roughly one-third of the transcripts for sugar-digesting enzymes in the entire midgut, exclusive of the proventriculus (Hixson et al., 2022).

All these findings in the previous literature together with our results could suggest that TKRP might have functions in lipid metabolism and digestive enzyme regulation, but no apparent role in bloodmeal digestion. These suggestions are supported by the results showing TKRP expression being the greatest in the anterior midgut rather than posterior midgut. Furthermore, there were no difference between TKRP immunoreactivity in the male and female gut, suggesting TKRP actions are unrelated to feeding on blood. This notion that TKRPs likely have no major role in blood-feeding physiology was strongly supported by the data which showed there was no difference in TKRP immunoreactivity before and after blood feeding in females.

This study could also suggest that these neuropeptides have some roles in nutrition compound digestion but mostly in nectar and sugar digestion as well as possibly food search behavior in the mosquito *Ae. aegypti*. There was a significant reduction in TKRP immunoreactivity in starved mosquitos in both males and females, and furthermore, the fact that we observed TKRP immunoreactivity in the late-stage larvae anterior midgut, but it was much lower in comparison to adults, that also supports this proposition. Mosquito larvae anterior midgut has roles in nutritional digestion, but larvae do not feed on sugar-rich food stuffs but on algae, organic waste, and microbes (Raya et al., 2009), so TKRP immunoreactivity is present in larvae anterior midgut, but not as strong as observed in adults.

4.3. *tk* knockout *Ae. aegypti* line generation using CRISPR/Cas9

CRISPR/Cas9 system has lately emerged as the most commonly utilized tool for genome engineering in a variety of organisms. The CRISPR/Cas9 system is ideal for multiplex genome editing due to its efficient and appropriate production of numerous guide RNAs (gRNAs) (Hsieh-Feng and Yang, 2020). During the past several years, different CRISPR/Cas9 expression

techniques or approaches have been utilized in arthropods, specifically in the mosquito *Ae. aegypti* including ReMOT Control and embryonic microinjection (Chaverra-Rodriguez et al., 2018; Kistler et al., 2015; Sun et al., 2022).

4.3.1 ReMOT Control

In the current results, transduced EGFP was found in yolk granules throughout oocyte development after injection of P2C-EGFP-Cas9. EGFP uptake was seen in all dissected ovaries 24 hours post injection but in 70% of dissected ovaries 18 hours post injection (Figure 3.8), indicating that the later time post injection is better suited for verifying EGFP uptake into the ovaries of dissecting animals. These results are consistent with findings reported earlier in *Ae. aegypti* and *D. melanogaster* (Chaverra-Rodriguez et al., 2018). P2C-Cas9 along with different sgRNAs directed against the *tk* gene (see Table. 2.1a) were administered to female mosquitoes; however, no mutations were observed upon screening. Consequently, I proceeded with embryonic microinjection as the next step in efforts to generate *tk* knockout mosquitoes.

In this secondary approach, we demonstrated the effective transmission of P2C-EGFP-Cas9 into the oocyte from haemolymph following injection. Through meticulous testing of sgRNAs in embryonic injection, we confirmed the functionality of our designed sgRNAs. However, in investigating potential challenges hindering the success of ReMOT technique, we identified the endosomal escape reagent as a critical factor. To address this issue and enhance the efficiency of the technique, we propose a troubleshooting strategy involving the optimization of various endosomal escape reagents at different concentrations. This systematic approach aims to pinpoint the optimal conditions for successful implementation, thereby advancing the overall effectiveness of the method.

4.3.2 Embryonic microinjection

For choosing the best sgRNA to inject, six sgRNA were designed and injected together (two sets of three sgRNA where the same primer pairs could be used in PCR screening for confirmation of mutants) into *Ae. aegypti* embryos. Injecting multiple sgRNAs increases editing efficiency since some areas of the genome are indeed more resistant to CRISPR/Cas9 editing. The likelihood of successful edits can get boosted by developing numerous sgRNAs that target distinct places within the same gene. Moreover, creating numerous sgRNAs and then choosing the most particular and effective ones can help limit the possibility of off-target effects (Hsieh-Feng and Yang, 2020).

After establishing sgRNA1 and 2 as the best candidate sgRNAs for the embryonic microinjections, sgRNA1 was injected into eggs and heterozygous *tk* mutant animals were achieved. Heterozygous mutants were outcrossed to wild type mosquitoes for three generations. Additional outcrossing by mating heterozygous mutants with a wild-type strain can improve the stability of the knockout line. Genetic drift and the accumulation of background mutations in knockout lines can occur over numerous generations. Outcrossing to a wild-type strain can dilute these background changes and bring the genetic background closer to the original wild type (Agrawal and Whitlock, 2011).

After three generations of outcrossing, individuals of the heterozygous *tk* mutant line were crossed together to achieve a homozygous *tk* mutant mosquito line. Following the identification of homozygous mutants on the gel, Sanger sequencing results (The Centre for Applied Genomics, Sick Kids, Toronto, ON) confirmed genetic modification of the *tk* gene. However, the genomic disruption resulted in a 6-nucleotide deletion (Figure 3.11), indicating that there was no change in the codon reading frame but instead, resulted in a two-amino acid truncation of the TKRP prepropeptide.

This was an unfortunate result, since the desired outcome was a frameshift mutation, which is a genetic change brought on by an insertion or deletion of nucleotides that changes how the mRNA sequence is translated. Codons consist of three nucleotides and are used to represent specific amino acids or stop signals in DNA (or RNA) nucleotide sequences. To create a chain of amino acids and a protein, the codon sequence is read sequentially from the nucleotide sequence during translation. Frameshift mutations occur when nucleotides are added or removed from the regular sequence of codons, provided that the number of nucleotides added or removed is not a multiple of three. For instance, if only one nucleotide is removed from the sequence, the reading frame will be disrupted for all codons after the mutation (Oetting et al., 1991). As a result, the protein may have a large number of erroneous amino acids. In contrast, there won't be a change in the codon reading frame if a sequence that is a multiple of three nucleotides are added or removed. Regardless of this result, immunohistochemistry was performed on homozygous *tk* mutant progeny and, as expected, TKRPs immunoreactivity was still observed in enteroendocrine cells throughout the mosquito midgut (Figure 3.12).

One plausible hypothesis could suggest that the *tk* mutation is potentially lethal, resulting in the death of homozygote mutants. To investigate this, a potential troubleshooting strategy involves designing sgRNAs specifically targeting TKRP 2-5 while sparing TKRP 1. This targeted genetic modification aims to preserve the production of TKRP1, potentially ensuring the mosquito's survival. By selectively eliminating the other members of the neuropeptide family, we can attenuate their collective function, facilitating a comprehensive study of their roles in mosquito biology.

4.4. Concluding remarks and future directions

This study showed the localization of TKRPs in the midgut of the mosquito *Ae. aegypti*. The data appears to demonstrate that the distribution of TKRP immunoreactivity in the midgut is greatest in the proventriculus and anterior midgut. There is also TKRP immunolocalized in the very anterior (frontal) and posterior (caudal) regions of the posterior midgut of the adult female and male mosquitoes. It has also been confirmed that, over the developmental stages examined in this study, TKRP immunoreactivity peaked in the adult stage. Moreover, there is a significant difference in TKRP immunoreactivity between sugar fed and starved mosquitoes, with the latter showing a marked reduction in TKRP staining. These results suggest that TKRPs may have roles mostly in the digestion of sucrose and nectar rather than functions related to the digestion of blood. In regard to this potential function of TKRPs, the roles of these peptides are still unclear in the mosquito *Ae. aegypti*. In this study, we designed some functional sgRNAs which in future studies can be used to reattempt creating a *tk* knockout line that can subsequently be used to better establish the role of this peptide family in this mosquito species. Moreover, homology directed repair (HDR) can also be utilized in the future to achieve *tk* knockout mosquitoes. More questions to be answered in future studies could be what are the distributions of TKRP immunoreactive neurons in the nervous system of *Ae. aegypti*? This question can be answered through utilizing immunohistochemistry on *Ae. aegypti* brain under different physiological conditions including feeding, satiety, starvation and developmental stage.

References:

- Adams, M. D., Celniker, S. E., Holt, R. A., Evans, C. A., Gocayne, J. D., Amanatides, P. G., Scherer, S. E., Li, P. W., Hoskins, R. A., Galle, R. F., et al.** (2000). The genome sequence of *Drosophila melanogaster*. *Science* **287**, 2185–2195.
- Adli, M.** (2018). The CRISPR tool kit for genome editing and beyond. *Nat. Commun.* **2018** *9*, 1–13.
- Agrawal, A. F. and Whitlock, M. C.** (2011). Inferences About the Distribution of Dominance Drawn From Yeast Gene Knockout Data. *Genetics* **187**, 553.
- Altstein, M. and Nässel, D. R.** (2010). Neuropeptide signaling in insects. *Adv. Exp. Med. Biol.* **692**, 155–165.
- Baldrige, D., Wangler, M. F., Bowman, A. N., Yamamoto, S., Schedl, T., Pak, S. C., Postlethwait, J. H., Shin, J., Solnica-Krezel, L., Bellen, H. J., et al.** (2021). Model organisms contribute to diagnosis and discovery in the undiagnosed diseases network: Current state and a future vision. *Orphanet J. Rare Dis.* **16**, 1–17.
- Barrangou, R. and Marraffini, L. A.** (2014). CRISPR-Cas systems: prokaryotes upgrade to adaptive immunity. *Mol. Cell* **54**, 234.
- Basu, S., Aryan, A., Overcash, J. M., Samuel, G. H., Anderson, M. A. E., Dahlem, T. J., Myles, K. M. and Adelman, Z. N.** (2015). Silencing of end-joining repair for efficient site-specific gene insertion after TALEN/CRISPR mutagenesis in *Aedes aegypti*. *Proc. Natl. Acad. Sci.* **112**, 4038–4043.
- Bhat, U. S., Shahi, N., Surendran, S. and Babu, K.** (2021). Neuropeptides and Behaviors:

How Small Peptides Regulate Nervous System Function and Behavioral Outputs. *Front. Mol. Neurosci.* **14**, 786471.

Bhattacharya, D. and Van Meir, E. G. (2019). A simple genotyping method to detect small CRISPR-Cas9 induced indels by agarose gel electrophoresis. *Sci. Reports 2019 91* **9**, 1–7.

Billingsley, P. F. (2003). The Midgut Ultrastructure of Hematophagous Insects. <http://dx.doi.org/10.1146/annurev.en.35.010190.001251> **35**, 219–248.

Billingsley, P. F. and Lehane, M. J. (1996). Structure and ultrastructure of the insect midgut. *Biol. Insect Midgut* 3–30.

Brockmann, A., Annangudi, S. P., Richmond, T. A., Ament, S. A., Xie, F., Southey, B. R., Rodriguez-Zas, S. R., Robinson, G. E. and Sweedler, J. V. (2009). Quantitative peptidomics reveal brain peptide signatures of behavior. *Proc. Natl. Acad. Sci. U. S. A.* **106**, 2383–2388.

Brown, M. R., Graf, R., Swiderek, K. M., Fendley, D., Stracker, T. H., Champagne, D. E. and Lea, A. O. (1998). Identification of a steroidogenic neurohormone in female mosquitoes. *J. Biol. Chem.* **273**, 3967–3971.

Brown, M. R., Crim, J. W., Arata, R. C., Cai, H. N., Chun, C. and Shen, P. (1999). Identification of a *Drosophila* brain-gut peptide related to the neuropeptide Y family. *Peptides* **20**, 1035–1042.

Bui, M., Dalla Benetta, E., Dong, Y., Zhao, Y., Yang, T., Li, M., Antoshechkin, I. A., Buchman, A., Bottino-Rojas, V., James, A. A., et al. (2023). CRISPR mediated transactivation in the human disease vector *Aedes aegypti*. *PLOS Pathog.* **19**, e1010842.

- Caccia, S., Casartelli, M. and Tettamanti, G.** (2019). The amazing complexity of insect midgut cells: types, peculiarities, and functions. *Cell Tissue Res.* **377**, 505–525.
- Caers, J., Verlinden, H., Zels, S., Vandersmissen, H. P., Vuerinckx, K. and Schoofs, L.** (2012). More than two decades of research on insect neuropeptide GPCRs: an overview. *Front. Endocrinol. (Lausanne)*. **3**,
- Champagne, D. E. and Ribeiro, J. M. C.** (1994). Sialokinin I and II: vasodilatory tachykinins from the yellow fever mosquito *Aedes aegypti*. *Proc. Natl. Acad. Sci. U. S. A.* **91**, 138.
- Chaverra-Rodriguez, D., Macias, V. M., Hughes, G. L., Pujhari, S., Suzuki, Y., Peterson, D. R., Kim, D., McKeand, S. and Rasgon, J. L.** (2018). Targeted delivery of CRISPR-Cas9 ribonucleoprotein into arthropod ovaries for heritable germline gene editing. *Nat. Commun.* **2018 91 9**, 1–11.
- Chen, X. G., Mathur, G. and James, A. A.** (2008). Gene expression studies in mosquitoes. *Adv. Genet.* **64**, 19–50.
- Christie, A. E., Lundquist, C. T., Nässel, D. R. and Nusbaum, M. P.** (1997). Two novel tachykinin-related peptides from the nervous system of the crab *Cancer borealis*. *J. Exp. Biol.* **200**, 2279–2294.
- Christophers, S.** (1960). *Aedes aegypti* (L.) the Yellow Fever Mosquito: its Life History, Bionomics and Structure. *Aedes aegypti Yellow Fever Mosq. its Life Hist. Bionomics Struct.*
- Clements, A. N. (Alan N. and Clements, A. N. (Alan N.** (1992). The biology of mosquitoes.
- Clemons, A., Haugen, M., Flannery, E., Tomchaney, M., Kast, K., Jacowski, C., Le, C., Mori, A., Holland, W. S., Sarro, J., et al.** (2010). *Aedes aegypti*: an Emerging Model for

Vector Mosquito Development. *Cold Spring Harb. Protoc.* **2010**, pdb.emol141.

- Cottrell, G. A., Davies, N. W. and Green, K. A.** (1984). Multiple actions of a molluscan cardioexcitatory neuropeptide and related peptides on identified *Helix* neurones. *J. Physiol.* **356**, 315–333.
- Cui, Y. and Franz, A. W. E.** (2020). Heterogeneity of midgut cells and their differential responses to blood meal ingestion by the mosquito, *Aedes aegypti*. *Insect Biochem. Mol. Biol.* **127**, 103496.
- Curry, W. J., Fairweather, I., Johnston, C. F., Halton, D. W. and Buchanan, K. D.** (1989). Immunocytochemical demonstration of vertebrate neuropeptides in the earthworm *Lumbricus terrestris* (Annelida, Oligochaeta). *Cell Tissue Res.* **257**, 577–586.
- Dai, L. and Adams, M. E.** (2009). Ecdysis triggering hormone signaling in the yellow fever mosquito *Aedes aegypti*. *Gen. Comp. Endocrinol.* **162**, 43–51.
- Dixon, D. P., Van Ekeris, L. and Linser, P. J.** (2017). Characterization of carbonic anhydrase 9 in the alimentary canal of *Aedes aegypti* and its relationship to homologous mosquito carbonic anhydrases. *Int. J. Environ. Res. Public Health* **14**,.
- Dolezal, T., Krejцова, G., Bajgar, A., Nedbalova, P. and Strasser, P.** (2019). Molecular regulations of metabolism during immune response in insects. *Insect Biochem. Mol. Biol.* **109**, 31–42.
- Donaldson, Z. R. and Young, L. J.** (2008). Oxytocin, vasopressin, and the neurogenetics of sociality. *Science* **322**, 900–904.
- Dong, S., Lin, J., Held, N. L., Clem, R. J., Passarelli, A. L. and Franz, A. W. E.** (2015).

Heritable CRISPR/Cas9-Mediated Genome Editing in the Yellow Fever Mosquito, *Aedes aegypti*. *PLoS One* **10**, e0122353.

Elphick, M. R., Mirabeau, O. and Larhammar, D. (2018). Evolution of neuropeptide signalling systems. *J. Exp. Biol.* **221**,

Erspamer, V. Erspamer, G. F. (1962). Pharmacological actions of eledoisin on extravascular smooth muscle. *Br. J. Pharmacol. Chemother.* **19**, 337–354.

Fónagy, A., Schoofs, L., Proost, P., Van Damme, J., Bueds, H. and De Loof, A. (1992).

Isolation, primary structure and synthesis of neomyosuppressin, a myoinhibiting neuropeptide from the grey fleshfly, *Neobellieria bullata*. *Comp. Biochem. Physiol. C.* **102**, 239–245.

Glantz, R. M., Miller, C. S. and Nässel, D. R. (2000). Tachykinin-Related Peptide and GABA-Mediated Presynaptic Inhibition of Crayfish Photoreceptors. *J. Neurosci.* **20**, 1780.

Gonatopoulos-Pournatzis, T., Aregger, M., Brown, K. R., Farhangmehr, S., Braunschweig, U., Ward, H. N., Ha, K. C. H., Weiss, A., Billmann, M., Durbic, T., et al. (2020). Genetic interaction mapping and exon-resolution functional genomics with a hybrid Cas9–Cas12a platform. *Nat. Biotechnol.* 2020 385 **38**, 638–648.

Gratz, S. J., Wildonger, J., Harrison, M. M. and O’Connor-Giles, K. M. (2013).

CRISPR/Cas9-mediated genome engineering and the promise of designer flies on demand. *Fly (Austin)*. **7**, 249–255.

Hai, T., Teng, F., Guo, R., Li, W. and Zhou, Q. (2014). One-step generation of knockout pigs by zygote injection of CRISPR/Cas system. *Cell Res.* 2014 243 **24**, 372–375.

- Hall, A. B., Basu, S., Jiang, X., Qi, Y., Timoshevskiy, V. A., Biedler, J. K., Sharakhova, M. V., Elahi, R., Anderson, M. A. E., Chen, X.-G., et al.** (2015). A male-determining factor in the mosquito *Aedes aegypti*. *Science* (80-.). **348**, 1268–1270.
- Hammond, A., Galizi, R., Kyrou, K., Simoni, A., Siniscalchi, C., Katsanos, D., Gribble, M., Baker, D., Marois, E., Russell, S., et al.** (2016). A CRISPR-Cas9 gene drive system targeting female reproduction in the malaria mosquito vector *Anopheles gambiae*. *Nat. Biotechnol.* 2015 341 **34**, 78–83.
- Hansen, K. K., Stafflinger, E., Schneider, M., Hauser, F., Cazzamali, G., Williamson, M., Kollmann, M., Schachtner, J. and Grimmelikhuijzen, C. J. P.** (2010). Discovery of a Novel Insect Neuropeptide Signaling System Closely Related to the Insect Adipokinetic Hormone and Corazonin Hormonal Systems *. *J. Biol. Chem.* **285**, 10736–10747.
- Hecker, H.** (1977). Structure and function of midgut epithelial cells in culicidae mosquitoes (insecta, diptera). *Cell Tissue Res.* **184**, 321–341.
- Helke, C. J., Krause, J. E., Mantyh, P. W., Couture, R. and Rannon, M. J.** (1990). Diversity in mammalian tachykinin peptidergic neurons: multiple peptides, receptors, and regulatory mechanisms¹. *FASEB J.* **4**, 1606–1615.
- Heo, Y. T., Quan, X., Xu, Y. N., Baek, S., Choi, H., Kim, N. H. and Kim, J.** (2015). CRISPR/Cas9 nuclease-mediated gene knock-in in bovine-induced pluripotent cells. *Stem Cells Dev.* **24**, 393–402.
- Hixson, B. tta, Bing, X. L., Yang, X., Bonfini, A., Nagy, P. and Buchon, N.** (2022). A transcriptomic atlas of *Aedes aegypti* reveals detailed functional organization of major body parts and gut regional specializations in sugar-fed and blood-fed adult females. *Elife* **11**,.

- Hökfelt, T., Barde, S., Xu, Z. Q. D., Kuteeva, E., Rüegg, J., Le Maitre, E., Risling, M., Kehr, J., Ihnatko, R., Theodorsson, E., et al.** (2018). Neuropeptide and small transmitter coexistence: Fundamental studies and relevance to mental illness. *Front. Neural Circuits* **12**, 106.
- Holzer, P. and Holzer-Petsche, U.** (1997). Tachykinins in the gut. Part I. Expression, release and motor function. *Pharmacol. Ther.* **73**, 173–217.
- Honda, A., Hirose, M., Sankai, T., Yasmin, L., Yuzawa, K., Honsho, K., Izu, H., Iguchi, A., Ikawa, M. and Ogura, A.** (2015). Single-step generation of rabbits carrying a targeted allele of the tyrosinase gene using CRISPR/Cas9. *Exp. Anim.* **64**, 31.
- Hsieh-Feng, V. and Yang, Y.** (2020). Efficient expression of multiple guide RNAs for CRISPR/Cas genome editing. *aBIOTECH* **1**, 123.
- Hsu, P. D., Lander, E. S. and Zhang, F.** (2014). Development and Applications of CRISPR-Cas9 for Genome Engineering. *Cell* **157**, 1262.
- Ignell, R., Root, C. M., Birse, R. T., Wang, J. W., Nässel, D. R. and Winther, Å. M. E.** (2009). Presynaptic peptidergic modulation of olfactory receptor neurons in *Drosophila*. *Proc. Natl. Acad. Sci. U. S. A.* **106**, 13070–13075.
- Jasinskiene, N., Juhn, J. and James, A. A.** (2007). Microinjection of *A. aegypti* Embryos to Obtain Transgenic Mosquitoes. *J. Vis. Exp.*
- Kahsai, L., Kapan, N., Dircksen, H., Winther, Å. M. E. and Nässel, D. R.** (2010). Metabolic Stress Responses in *Drosophila* Are Modulated by Brain Neurosecretory Cells That Produce Multiple Neuropeptides. *PLoS One* **5**, e11480.

- Kanchiswamy, C. N., Maffei, M., Malnoy, M., Velasco, R. and Kim, J. S.** (2016). Fine-Tuning Next-Generation Genome Editing Tools. *Trends Biotechnol.* **34**, 562–574.
- Kauffman, E. B. and Kramer, L. D.** (2017). Zika Virus Mosquito Vectors: Competence, Biology, and Vector Control. *J. Infect. Dis.* **216**, S976–S990.
- Kaufmann, C. and Brown, M. R.** (2006). Adipokinetic hormones in the African malaria mosquito, *Anopheles gambiae*: Identification and expression of genes for two peptides and a putative receptor. *Insect Biochem. Mol. Biol.* **36**, 466–481.
- Kistler, K. E., Vosshall, L. B. and Matthews, B. J.** (2015). Genome-engineering with CRISPR-Cas9 in the mosquito *Aedes aegypti*. *Cell Rep.* **11**, 51.
- Ko, K. I., Root, C. M., Lindsay, S. A., Zaninovich, O. A., Shepherd, A. K., Wasserman, S. A., Kim, S. M. and Wang, J. W.** (2015). Starvation promotes concerted modulation of appetitive olfactory behavior via parallel neuromodulatory circuits. *Elife* **4**,.
- Kwok, R., Chung, D., Brugge, V. Te and Orchard, I.** (2005). The distribution and activity of tachykinin-related peptides in the blood-feeding bug, *Rhodnius prolixus*. *Peptides* **26**, 43–51.
- Lander, E. S.** (2016). The Heroes of CRISPR. *Cell* **164**, 18–28.
- Larhammar, D.** (2009). Neuropeptides Phylogeny and Evolution. *Encycl. Neurosci.* 873–880.
- Li, Y., Hernandez-Martinez, S., Fernandez, F., Mayoral, J. G., Topalis, P., Priestap, H., Perez, M., Navare, A. and Noriega, F. G.** (2006). Biochemical, molecular, and functional characterization of PISCF-allatostatin, a regulator of juvenile hormone biosynthesis in the mosquito *Aedes aegypti*. *J. Biol. Chem.* **281**, 34048–34055.

- Lopes, T. F., Holcman, M. M., Barbosa, G. L., Domingos, M. de F. and Barreiros, R. M. O. V.** (2014). Laboratory evaluation of the development of *Aedes aegypti* in two seasons: influence of different place and different densities. *Rev. Inst. Med. Trop. Sao Paulo* **56**, 369.
- Macias, V. M., McKeand, S., Chaverra-Rodriguez, D., Hughes, G. L., Fazekas, A., Pujhari, S., Jasinskiene, N., James, A. A. and Rasgon, J. L.** (2020). Cas9-Mediated Gene-Editing in the Malaria Mosquito *Anopheles stephensi* by ReMOT Control. *G3 Genes|Genomes|Genetics* **10**, 1353–1360.
- Mains, R. E. and Eipper, B. A.** (1999). The Neuropeptides. **Martin-Martin, I., Aryan, A., Meneses, C., Adelman, Z. N. and Calvo, E.** (2018). Optimization of sand fly embryo microinjection for gene editing by CRISPR/Cas9. *PLoS Negl. Trop. Dis.* **12**,.
- Matsumoto, S., Brown, M. R., Crim, J. W., Vigna, S. R. and Lea, A. O.** (1989). Isolation and primary structure of neuropeptides from the mosquito, *Aedes aegypti*, immunoreactive to FMRFamide antiserum. *Insect Biochem.* **19**, 277–283.
- McKenzie, A. T., Wang, M., Hauberg, M. E., Fullard, J. F., Kozlenkov, A., Keenan, A., Hurd, Y. L., Dracheva, S., Casaccia, P., Roussos, P., et al.** (2018). A practical guide to genome-engineering with CRISPR-Cas9 in the mosquito *Aedes aegypti*. *Sci. Rep.* **8**, 8868.
- McMeniman, C. J., Corfas, R. A., Matthews, B. J., Ritchie, S. A. and Vosshall, L. B.** (2014). Multimodal integration of carbon dioxide and other sensory cues drives mosquito attraction to humans. *Cell* **156**, 1060–1071.
- Mishra, A. and Lal, G.** (2021). Neurokinin receptors and their implications in various autoimmune diseases. *Curr. Res. Immunol.* **2**, 66.

- Mizoguchi, A. and Okamoto, N.** (2013). Insulin-like and IGF-like peptides in the silkworm *Bombyx mori*: Discovery, structure, secretion, and function. *Front. Physiol.* **4** AUG, 60896.
- Muren, J. E. and Nässel, D. R.** (1996). Isolation of five tachykinin-related peptides from the midgut of the cockroach *Leucophaea maderae*: existence of N-terminally extended isoforms. *Regul. Pept.* **65**, 185–196.
- Muren, J. E. and Nässel, D. R.** (1997). Seven tachykinin-related peptides isolated from the brain of the Madeira cockroach: evidence for tissue-specific expression of isoforms. *Peptides* **18**, 7–15.
- Musso, P. Y., Junca, P. and Gordon, M. D.** (2021). A neural circuit linking two sugar sensors regulates satiety-dependent fructose drive in *Drosophila*. *Sci. Adv.* **7**, 186.
- Nachman, R. J., Holman, G. M., Haddon, W. F. and Ling, N.** (1986). Leucosulfakinin, a Sulfated Insect Neuropeptide with Homology to Gastrin and Cholecystokinin. *Science* (80-). **234**, 71–73.
- Nachman, R. J., Moyna, G., Williams, H. J., Zabrocki, J., Zadina, J. E., Coast, G. M. and Vanden Broeck, J.** (1999). Comparison of active conformations of the insectatachykinin/tachykinin and insect kinin/Tyr-W-MIF-1 neuropeptide family pairs. *Ann. N. Y. Acad. Sci.* **897**, 388–400.
- Nässel, D. R.** (1999). Tachykinin-related peptides in invertebrates: a review. *Peptides* **20**, 141–158.
- Nässel, D. R. and Winther, M. E. A.** (2002). Neuronal co-localization of different isoforms of tachykinin-related peptides (LemTRPs) in the cockroach brain. *Cell Tissue Res.* **308**, 225–

- Nässel, D. R., Zandawala, M., Kawada, T. and Satake, H.** (2019). Tachykinins: Neuropeptides That Are Ancient, Diverse, Widespread and Functionally Pleiotropic. *Front. Neurosci.* **13**, 1262.
- Nene, V., Wortman, J. R., Lawson, D., Haas, B., Kodira, C., Tu, Z., Loftus, B., Xi, Z., Megy, K., Grabherr, M., et al.** (2007). Genome sequence of *Aedes aegypti*, a major arbovirus vector. *Science* **316**, 1718–1723.
- Ni, W., Qiao, J., Hu, S., Zhao, X., Regouski, M., Yang, M., Polejaeva, I. A. and Chen, C.** (2014). Efficient Gene Knockout in Goats Using CRISPR/Cas9 System. *PLoS One* **9**, e106718.
- Noonan, J. P., Coop, G., Kudaravalli, S., Smith, D., Krause, J., Alessi, J., Chen, F., Platt, D., Pääbo, S., Pritchard, J. K., et al.** (2006). Sequencing and Analysis of Neanderthal Genomic DNA. *Science* **314**, 1113.
- Oetting, W. S., Mentink, M. M., Symmers, C. G., Lewis, R. A., White, J. G. and King, R. A.** (1991). Three different frameshift mutations of the tyrosinase gene in type IA oculocutaneous albinism. *Am. J. Hum. Genet.* **49**, 199.
- Pauls, D., Chen, J., Reiher, W., Vanselow, J. T., Schlosser, A., Kahnt, J. and Wegener, C.** (2014). Peptidomics and processing of regulatory peptides in the fruit fly *Drosophila*. *EuPA Open Proteomics* **3**, 114–127.
- Poels, J., Birse, R. T., Nachman, R. J., Fichna, J., Janecka, A., Vanden Broeck, J. and Nässel, D. R.** (2009). Characterization and distribution of NKD, a receptor for *Drosophila*

- tachykinin-related peptide 6. *Peptides* **30**, 545–556.
- Powell, J. R. and Tabachnick, W. J.** (2013). History of domestication and spread of *Aedes aegypti* - A Review. *Mem. Inst. Oswaldo Cruz* **108**, 11.
- Predel, R., Neupert, S., Garczynski, S. F., Crim, J. W., Brown, M. R., Russell, W. K., Kahnt, J., Russell, D. H. and Nachman, R. J.** (2010). Neuropeptidomics of the mosquito *Aedes aegypti*. *J. Proteome Res.* **9**, 2006–2015.
- Purves, D., Augustine, G. J., Fitzpatrick, D., Katz, L. C., LaMantia, A.-S., McNamara, J. O. and Williams, S. M.** (2001). Peptide Neurotransmitters.
- Raminani, L. N. and Cupp, E. W.** (1975). Early embryology of *Aedes aegypti* (L.) (Diptera: Culicidae). *Int. J. Insect Morphol. Embryol.* **4**, 517–528.
- Ran, F. A., Hsu, P. D., Wright, J., Agarwala, V., Scott, D. A. and Zhang, F.** (2013). Genome engineering using the CRISPR-Cas9 system. *Nat. Protoc.* **2013 811 8**, 2281–2308.
- Raya, K., Mercedes, M., Chan, D., Choi, C. Y. and Nishiura, J. T.** (2009). Growth and differentiation of the larval mosquito midgut. *J. Insect Sci.* **9**, 1536–2442.
- Ribeiro, J. M.** (1992). Characterization of a Vasodilator from the Salivary Glands of the Yellow Fever Mosquito *Aedes aegypti*. *J. Exp. Biol.* **165**, 61–71.
- Riehle, M. A., Fan, Y., Cao, C. and Brown, M. R.** (2006). Molecular characterization of insulin-like peptides in the yellow fever mosquito, *Aedes aegypti*: expression, cellular localization, and phylogeny. *Peptides* **27**, 2547–2560.
- Sajadi, F. and Paluzzi, J. P. V.** (2021). Hormonal regulation and functional role of the “renal” tubules in the disease vector, *Aedes aegypti*. *Vitam. Horm.* **117**, 189–225.

- Sanders, H. R., Evans, A. M., Ross, L. S. and Gill, S. S.** (2003). Blood meal induces global changes in midgut gene expression in the disease vector, *Aedes aegypti*. *Insect Biochem. Mol. Biol.* **33**, 1105–1122.
- Satake, H., Takuwa, K., Minakata, H. and Matsushima, O.** (1999). Evidence for Conservation of the Vasopressin/Oxytocin Superfamily in Annelida. *J. Biol. Chem.* **274**, 5605–5611.
- Schoofs, L., Holman, G. M., Hayes, T. K., Nachman, R. J. and De Loof, A.** (1990a). Locustatachykinin I and II, two novel insect neuropeptides with homology to peptides of the vertebrate tachykinin family. *FEBS Lett.* **261**, 397–401.
- Schoofs, L., Holman, G. M., Hayes, T. K., Kochansky, J. P., Nachman, R. J. and De Loof, A.** (1990b). Locustatachykinin III and IV: two additional insect neuropeptides with homology to peptides of the vertebrate tachykinin family. *Regul. Pept.* **31**, 199–212.
- Sehadova, H., Takasu, Y., Zaloudikova, A., Lin, Y. H., Sauman, I., Sezutsu, H., Rouhova, L., Kodrik, D. and Zurovec, M.** (2020). Functional Analysis of Adipokinetic Hormone Signaling in *Bombyx mori*. *Cells* **9**,.
- Severini, C., Improta, G., Falconieri-Erspamer, G., Salvadori, S. and Erspamer, V.** (2002). The tachykinin peptide family. *Pharmacol. Rev.* **54**, 285–322.
- Severson, D. W., Knudson, D. L., Soares, M. B. and Loftus, B. J.** (2004). *Aedes aegypti* genomics. *Insect Biochem. Mol. Biol.* **34**, 715–721.
- Singer, M. and Frischknecht, F.** (2017). Time for Genome Editing: Next-Generation Attenuated Malaria Parasites. *Trends Parasitol.* **33**, 202–213.

Soghigian, J., Gloria-Soria, A., Robert, V., Le Goff, G., Failloux, A. B. and Powell, J. R.

(2020). Genetic evidence for the origin of *Aedes aegypti*, the yellow fever mosquito, in the southwestern Indian Ocean. *Mol. Ecol.* **29**, 3593.

Song, W., Veenstra, J. A. and Perrimon, N. (2014). Control of lipid metabolism by Tachykinin in *Drosophila*. *Cell Rep.* **9**, 40.

Steinhoff, M. S., von Mentzer, B., Geppetti, P., Pothoulakis, C. and Bunnett, N. W. (2014).

Tachykinins and Their Receptors: Contributions to Physiological Control and the Mechanisms of Disease. *Physiol. Rev.* **94**, 265.

Sun, R., Li, M., McMeniman, C. J. and Akbari, O. S. (2022). CRISPR-Mediated Genome Engineering in *Aedes aegypti*. *Methods Mol. Biol.* **2509**, 23–51.

Terhzaz, S., O’Connell, F. C., Pollock, V. P., Kean, L., Davies, S. A., Veenstra, J. A. and Dow, J. A. T. (1999). Isolation and characterization of a leucokinin-like peptide of *Drosophila melanogaster*. *J. Exp. Biol.* **202**, 3667–3676.

Uddin, F., Rudin, C. M. and Sen, T. (2020). CRISPR Gene Therapy: Applications, Limitations, and Implications for the Future. *Front. Oncol.* **10**, 541550.

Urbański, A., Johnston, P., Bittermann, E., Keshavarz, M., Paris, V., Walkowiak-Nowicka, K., Konopińska, N., Marciniak, P. and Rolff, J. (2022). Tachykinin-related peptides modulate immune-gene expression in the mealworm beetle *Tenebrio molitor* L. *Sci. Reports* **2022 121 12**, 1–19.

v. Euler, U. S. and Gaddum, J. H. (1931). An unidentified depressor substance in certain tissue extracts. *J. Physiol.* **72**, 74.

- Veenstra, J. A.** (1988). Immunocytochemical demonstration of vertebrate peptides in invertebrates: The homology concept. *Neuropeptides* **12**, 49–54.
- Veenstra, J. A.** (1994). Isolation and Identification of 3 Leucokinins from the Mosquito *Aedes aegypti*. *Biochem. Biophys. Res. Commun.* **202**, 715–719.
- Veenstra, J. A. and Costes, L.** (1999). Isolation and identification of a peptide and its cDNA from the mosquito *Aedes aegypti* related to *Manduca sexta* allatotropin. *Peptides* **20**, 1145–1151.
- Veenstra, J. A., Lau, G. W., Agricola, H. J. and Petzel, D. H.** (1995). Immunohistological localization of regulatory peptides in the midgut of the female mosquito *Aedes aegypti*. *Histochem. Cell Biol.* **104**, 337–347.
- Veenstra, J. A., Noriega, F. G., Graf, R. and Feyereisen, R.** (1997). Identification of three allatostatins and their cDNA from the mosquito *Aedes aegypti*. *Peptides* **18**, 937–942.
- Wahedi, A., Gäde, G. and Paluzzi, J. P.** (2019). Insight Into Mosquito GnRH-Related Neuropeptide Receptor Specificity Revealed Through Analysis of Naturally Occurring and Synthetic Analogs of This Neuropeptide Family. *Front. Endocrinol. (Lausanne)*. **10**,.
- Wang, Y., Li, Z., Xu, J., Zeng, B., Ling, L., You, L., Chen, Y., Huang, Y. and Tan, A.** (2013). The CRISPR/Cas system mediates efficient genome engineering in *Bombyx mori*. *Cell Res.* **23**, 1414–1416.
- Wang, H., La Russa, M. and Qi, L. S.** (2016). CRISPR/Cas9 in Genome Editing and Beyond. *Annu. Rev. Biochem.* **85**, 227–264.
- Watts, D. M., Burke, D. S., Harrison, B. A., Whitmire, R. E. and Nisalak, A.** (1987). Effect

of temperature on the vector efficiency of *Aedes aegypti* for dengue 2 virus. *Am. J. Trop. Med. Hyg.* **36**, 143–152.

Whitton, C., Daub, J., Quail, M., Hall, N., Foster, J., Ware, J., Ganatra, M., Slatko, B., Barrell, B. and Blaxter, M. (2004). A genome sequence survey of the filarial nematode *Brugia malayi*: repeats, gene discovery, and comparative genomics. *Mol. Biochem. Parasitol.* **137**, 215–227.

Winther, Å. M. E., Siviter, R. J., Isaac, R. E., Predel, R. and Nässel, D. R. (2003). Neuronal expression of tachykinin-related peptides and gene transcript during postembryonic development of *Drosophila*. *J. Comp. Neurol.* **464**, 180–196.

Winther, Å. M. E., Acebes, A. and Ferrús, A. (2006). Tachykinin-related peptides modulate odor perception and locomotor activity in *Drosophila*. *Mol. Cell. Neurosci.* **31**, 399–406.

Wu, Z., Yang, L., He, Q. and Zhou, S. (2021). Regulatory Mechanisms of Vitellogenesis in Insects. *Front. Cell Dev. Biol.* **8**, 1863.

Wulff, J. P., Capriotti, N. and Ons, S. (2018). Orcokininins regulate the expression of neuropeptide precursor genes related to ecdysis in the hemimetabolous insect *Rhodnius prolixus*. *J. Insect Physiol.* **108**, 31–39.

Zhang, Y., Zhao, B., Roy, S., Saha, T. T., Kokoza, V. A., Li, M. and Raikhel, A. S. (2016). microRNA-309 targets the Homeobox gene SIX4 and controls ovarian development in the mosquito *Aedes aegypti*. *Proc. Natl. Acad. Sci.* **113**, E4828–E4836.

Zhang, J., Yang, W., Xu, J., Yang, W., Li, Q., Zhong, Y., Cao, Y., Yu, X. Q. and Deng, X. (2018). Regulation of antimicrobial peptide genes via insulin-like signaling pathway in the

silkworm *Bombyx mori*. *Insect Biochem. Mol. Biol.* **103**, 12–21.

Zhang, S., Guo, F., Yan, W., Dai, Z., Dong, W., Zhou, J., Zhang, W., Xin, F. and Jiang, M.

(2020). Recent Advances of CRISPR/Cas9-Based Genetic Engineering and Transcriptional Regulation in Industrial Biology. *Front. Bioeng. Biotechnol.* **7**, 495345.